SMALL AMPLITUDE OSCILLATORY FORCING ON TWO-LAYER PLANE CHANNEL FLOW

By

Adrian V. Coward

and

Yuriko Y. Renardy

IMA Preprint Series # 1392

March 1996

INSTITUTE FOR MATHEMATICS AND ITS APPLICATIONS

UNIVERSITY OF MINNESOTA

514 Vincent Hall
206 Church Street S.E.
Minneapolis, Minnesota 55455

Small Amplitude Oscillatory Forcing on Two-Layer Plane Channel Flow

Adrian V. Coward
and
Yuriko Y. Renardy
Department of Mathematics and ICAM
Virginia Polytechnic Institute and State University
Blacksburg,
Virginia 24061-0123
U.S.A.

Abstract

The effect of oscillatory forcing as a dynamic stabilization or destabilization mechanism for two layer plane Couette-Poiseuille flow at low Reynolds number is studied using numerical and asymptotic methods. The flow is driven by the relative planar motion of the upper boundary and a pressure gradient in the streamwise direction. Both driving forces are composed of a steady part and small amplitude time-periodic fluctuations. An asymptotic expansion for the growth rates for small amplitudes is developed and the correction terms are quadratic in the amplitudes. The modulations to the steady flow can have either a stabilizing or destabilizing influence depending upon the conditions of flow. Complete stabilization is possible for certain flows which are otherwise unstable due to the viscosity stratification across the interface. The combined pressure and velocity fluctuations can have an opposite effect on the flow stability to that induced by the separate time-periodic forcing mechanisms.

1 Introduction

In flows of two immiscible liquids (see Chapter 1 of Joseph & Renardy 1993, Aminataei *et al.* 1988, Ranjbaran & Khomami 1995, Renardy 1995), studying the stability of the interface aids the understanding of the optimum flux conditions and can be used to help maintain a desired flow configuration. A two-layer flow may be unstable if the viscosities of the two fluids are different (Yih 1967). When the more viscous fluid occupies the thinner layer, the interfacial mode is unstable, whereas converse arrangements may be linearly stable to long waves leading to a thin-layer effect (Hooper 1985, Renardy 1987). Surface tension has a negligible effect on long wavelength disturbances but is important for short waves (Hooper & Boyd 1983, Hinch 1984). General wavelength disturbances are investigated by Renardy (1985), who shows examples of maximum growth rates attained for $O(1)$ waves. Renardy (1987) carried out an analytical study for fluids with slightly different mechanical properties, showing the explicit dependence of the eigenvalues on the parameters. Tilley, Davis & Bankoff (1994a,b) and Chen & Aidun (1994) considered two-layer flows down an inclined channel for long wavelength disturbances. In the case of a density difference the inclined problem differs from the plane Couette-Poiseuille flow in that the driving pressure gradients, which involve gravity, are different in each fluid. In the absence of gravity, the two problems are identical.

The inclusion of an oscillatory component to the steady flow can enhance or reduce stability (Grosch & Salwen 1968, Hall 1975, von Kerczek 1982, Davis 1975, Kelly & Hu 1993, Hu & Kelly 1995). Yih (1968) considered the stability of a viscous fluid layer on a flat plate performing a simple harmonic motion in its own plane. There is no viscosity coupling between the fluid and the air layer above. In the absence of plate oscillations, the mean flow is zero, and the flow is linearly stable. Using Floquet theory, he showed that the imposed oscillations can cause long wavelength disturbances to become unstable. This was extended by von Kerczek (1987) in a study of the flow down a vertical plate which is performing a simple harmonic motion in its own plane. Using a similar longwave expansion, von Kerczek established windows of stability.

Coward, Papageorgiou & Smyrlis (1995) studied the core-annular flow of two fluids in a vertical pipe. An oscillatory pressure gradient drives the flow in the axial direction. They obtained an evolution equation which describes

the temporal development of the interface position for axisymmetric disturbances to the base flow. They show that the inclusion of the time-periodic component gives rise to quasi-periodic traveling waves which move in the streamwise direction. Coward & Papageorgiou (1994) considered the flow of two superposed fluids between parallel plates, one of which oscillates in the streamwise direction. They used an approach similar to that of Yih (1968) to consider the overall growth or decay of long wavelength perturbations over a complete period of the forced boundary oscillations. The authors obtained an explicit formula for the Floquet exponent. This can be positive, zero, or negative and indicates how the various physical parameters cause the disturbances to the time-periodic flow to grow, remain neutral, or decay. Such a methodology is in contrast to a quasi-static approach in which time is treated as a parameter and instability is determined by considering all parametrized profiles. Coward & Papageorgiou showed that the oscillatory forcing of two-layer plane Couette flow can either stabilize or destabilize the long wavelength perturbations. They obtained representative results which show how an unstable interface can be completely stabilized by the time-periodic motion of the upper boundary.

In this investigation we extend the work of Coward & Papageorgiou (1994) in two ways. First, we consider disturbances of arbitrary wavenumber. Secondly, we consider the inclusion of a streamwise pressure gradient which contains a steady component and a time oscillatory part which may have a phase shift from the oscillations imposed on the bounding upper plate. In §2 we present the base solution for oscillatory plane Couette-Poiseuille flow. We derive the momentum equations governing the stability of the flow together with the appropriate boundary and interface conditions (Appendix). We restrict our investigation to the case when the oscillations have small amplitude. This enables us to use a Floquet theory to calculate the overall growth or decay of disturbances over a complete oscillation cycle. In §3 we describe the numerical scheme used to solve the stability problem. In §4 we consider the case when perturbations to the base flow have asymptotically long and short wavelengths. We derive closed form expressions for the growth rates of the interfacial mode, which we compare and verify with our results given by the numerical method. In §5, we show results for general wavenumber disturbances. Our conclusions are given in §6. Since the oscillation amplitude is assumed to be small, and the effect on the growth rate is proportional to the square of the oscillation amplitude, our numerical results show small

effects. However, the results show trends that may persist for larger values of the oscillation amplitude where this analysis cannot be done. In particular, we show that for a thin lubricating layer, the results on differences in layer thickness may be significant.

2 Equations Governing the Two-Layer Flow

Two fluids of densities ρ_i (i=1,2), and viscosities μ_i lie in layers between infinite parallel plates located at $z^* = 0, l^*$. Asterisks are used for dimensional variables. The lower plate is at rest. The upper plate moves in its plane with a steady velocity $(U_u^*, 0, 0)$ together with superposed sinusoidal oscillations of magnitude Δ_v^*. At a given time t^*, the upper boundary has velocity $U_u^* + \Delta_v^* \cos(\omega^* t^*)$. In the basic flow, fluid 1 occupies the region $0 \le z^* \le l_1^*$ and fluid 2 occupies $l_1^* \le z^* \le l^*$. The steady velocity at the interface in the basic flow is $(U^*(z^* = l_1^*), 0)$ and for brevity, we denote $U^*(z^* = l_1^*)$ by U_i. The velocity, distance, time and pressure are made dimensionless with respect to U_i, l^*, l^*/U_i, and $\rho_1 U_i^2$. The basic plane Couette-Poiseuille flow has a streamwise pressure gradient $-G^* + \Delta_p^* \cos(\omega^* t^* - \delta)$ in the x-direction. Reynolds numbers in each fluid are denoted by $R_1 = U_i l^* \rho_1/\mu_1$ and $R_2 = U_i l^* \rho_2/\mu_2$. There are seven dimensionless parameters which quantify the steady flow: a Reynolds number, say R_1, the undisturbed depth l_1 of fluid 1, a surface tension parameter T =(surface tension coefficient)$/(\mu_2 U_i)$, a Froude number F given by $F^2 = U_i^2/gl^*$ where g is the gravitational acceleration constant, a dimensionless pressure gradient $G = G^* l^*/(\rho_1 U_i^2)$, the viscosity ratio $m = \mu_1/\mu_2$, and a density ratio $r = \rho_1/\rho_2$. In addition, we define four further dimensionless parameters: the phase shift δ, the frequency of the imposed oscillations $\omega = \omega^* l^*/U_i$, and the magnitudes of the velocity and pressure modulations $\Delta_v = \Delta_v^*/U_i$ and $\Delta_p = \Delta_p^* l^*/(\rho_1 U_i^2)$. It is convenient here also to define parameters related to the Stokes layer thickness in each fluid: $\beta_1 = l^* (i\omega^* \rho_1/\mu_1)^{1/2} = (i\omega R_1)^{1/2}$, and $\beta_2 = l^* (i\omega^* \rho_2/\mu_2)^{1/2} = (i\omega R_2)^{1/2}$. The dimensionless basic flow $(U(z,t), 0)$ satisfies the Navier-Stokes equations

$$\frac{\partial U}{\partial t} = \frac{1}{R_i}\frac{\partial^2 U}{\partial z^2} + \frac{\rho_1 G}{\rho_i} - \frac{\rho_1 \Delta_p}{\rho_i}\cos(\omega t - \delta), \quad \frac{\partial P}{\partial z} = -\frac{\rho_i}{\rho_1 F^2},$$

where $i = 1$ denotes the lower layer $0 \le z \le l_1$, and $i = 2$ denotes the upper layer $l_1 \le z \le 1$. The no-slip velocity conditions are imposed at the solid

boundaries: $U(0,t)=0$, $U(1,t)=U_u+\Delta_v\cos(\omega t)$. At the interface the velocity $U(z=l_1,t)$ and tangential stress $\mu_i\partial U/\partial z$ are continuous. Separating the steady and unsteady components of the basic flow we have

$$\begin{aligned} U(z,t) &= U_s(z)+\frac{1}{2}\left\{\left[\Delta_v U_v+\Delta_p U_p e^{-i\delta}\right](z)\,e^{i\omega t}+c.c.\right\}, \\ U_s(z) &= \begin{cases} -GR_1z^2/2+c_1z, & 0\le z\le l_1, \\ -rGR_2(z-1)^2/2+c_2(z-1)+U_u, & l_1\le z\le 1, \end{cases} \end{aligned}$$

where $c.c.$ denotes the complex conjugate, $U_u=1+(ml_2)/l_1-(ml_2GR_1/2)$ the steady upper plate speed, $l_2=1-l_1$, $c_1=(1/l_1)+(GR_1l_1/2)$, and $c_2=m(c_1-GR_1)$. The components of the basic flow due to the oscillatory plate motion and forced pressure fluctuations can be written as follows.

$$\begin{aligned} U_v(z) &= \begin{cases} d_3\sinh(\beta_1 z), & 0\le z\le l_1, \\ [\cosh(\beta_2(z-1))+d_4\sinh(\beta_2(z-1))], & l_1\le z\le 1, \end{cases} \\ U_p(z) &= \begin{cases} (i\omega)^{-1}[\cosh(\beta_1 z)-1+d_1\sinh(\beta_1 z)], & 0\le z\le l_1, \\ (i\omega)^{-1}[r\cosh(\beta_2(z-1))-r+d_2\sinh(\beta_2(z-1))], & l_1\le z\le 1, \end{cases} \\ d_1 &= [(1-r)\cosh(\beta_2 l_2)+r-\cosh(\beta_1 l_1)\cosh(\beta_2 l_2) \\ &- (mr)^{1/2}\sinh(\beta_1 l_1)\sinh(\beta_2 l_2)]\,d_3, \\ d_2 &= [(mr)^{1/2}[r\cosh(\beta_1 l_1)\cosh(\beta_2 l_2)+(1-r)\cosh(\beta_1 l_1)-1] \\ &+ r\sinh(\beta_1 l_1)\sinh(\beta_2 l_2)]\,d_3, \\ d_3 &= [\sinh(\beta_1 l_1)\cosh(\beta_2 l_2)+(mr)^{1/2}\cosh(\beta_1 l_1)\sinh(\beta_2 l_2)]^{-1}, \\ d_4 &= [\sinh(\beta_1 l_1)\sinh(\beta_2 l_2)+(mr)^{1/2}\cosh(\beta_1 l_1)\cosh(\beta_2 l_2)]\,d_3. \end{aligned}$$

Solutions that are small perturbations of the above basic flow are sought. The velocity, pressure and interface position are perturbed by $(\tilde{u},\tilde{w})$, $\tilde{p}$, and $\tilde{h}$ respectively. Further we use Fourier mode expansions of the form

$$\begin{aligned} (\tilde{u},\tilde{w},\tilde{p})(x,z,t) &= \frac{1}{2}\left\{(u,w,p)(z,t)\,e^{i\alpha x+\sigma t}+c.c.\right\}, \\ \tilde{h}(x,t) &= \frac{1}{2}\left\{h(t)\,e^{i\alpha x+\sigma t}+c.c.\right\}. \end{aligned}$$

We use Floquet theory to derive and solve the eigenrelation for the complex eigenvalue σ. The flow is linearly stable to disturbances with streamwise

wavenumbers α (for given values of the eleven flow parameters) if σ has a negative real part.

After neglecting small nonlinear convective terms and eliminating u and p, the linearized Navier-Stokes equations and equation of continuity reduce to the familiar Orr-Sommerfeld equation

$$\begin{aligned} \frac{1}{R_i}\left(\frac{\partial^4}{\partial z^4} - 2\alpha^2\frac{\partial^2}{\partial z^2} + \alpha^4\right) w \;&-\; \left(i\alpha U + \frac{\partial}{\partial t}\right)\left(\frac{\partial^2}{\partial z^2} - \alpha^2\right) w \\ + i\alpha w\frac{\partial^2 U}{\partial z^2} \;&=\; \sigma\left(\frac{\partial^2 w}{\partial z^2} - \alpha^2 w\right). \end{aligned} \tag{1}$$

The no-slip boundary conditions $w = \partial w/\partial z = 0$ are imposed at the upper and lower plates $z = 0, 1$. The conditions at the interface are posed at the unknown position $z = l_1 + \tilde{h}$. Since the $\tilde{h}(t)$ is assumed to be small, the interfacial conditions are expanded as Taylor series about the unperturbed position $z = l_1$. Using the notation $[\![x]\!] \equiv x$(fluid 1) - x(fluid 2), evaluated at $z = l_1$, the continuity of velocity and shear stress across the interface are

$$[\![w]\!] = 0, \qquad i\alpha h[\![\frac{\partial U}{\partial z}]\!] - [\![\frac{\partial w}{\partial z}]\!] \;=\; 0, \tag{2a}$$

$$[\![\frac{\mu}{\mu_1}\left(\frac{\partial^2 w}{\partial z^2} + \alpha^2 w - i\alpha h\frac{\partial^2 U}{\partial z^2}\right)]\!] \;=\; 0, \tag{2b}$$

where μ denotes μ_i for fluid $i = 1, 2$. The balance of normal stress yields

$$\begin{aligned} [\![\frac{\mu}{\mu_1 R_1}\left(3\alpha^2\frac{\partial w}{\partial z} - \frac{\partial^3 w}{\partial z^3}\right)]\!] + \frac{\alpha^4 hT}{mR_1} + \frac{h\alpha^2(r-1)}{rF^2} \;&+ \\ [\![\frac{\rho}{\rho_1}\left(\sigma\frac{\partial w}{\partial z} + \frac{\partial^2 w}{\partial t\partial z} - i\alpha w\frac{\partial U}{\partial z} + i\alpha U\frac{\partial w}{\partial z}\right)]\!] \;&=\; 0. \end{aligned} \tag{2c}$$

Finally, the kinematic free surface condition gives

$$\frac{dh}{dt} + \sigma h + i\alpha hU - w \;=\; 0, \qquad \text{evaluated at } z = l_1. \tag{2d}$$

Our aim here is to quantify the stabilizing or destabilizing effect of the time-periodic pressure gradient and boundary motion on the otherwise steady two layer flow. To this end, we now take $\Delta_v, \Delta_p \ll 1$ and express the

eigenvalue σ and the perturbed flow as asymptotic expansions in these two small parameters.

$$\sigma = \sigma_s + \Delta_v^2\sigma_{v2} + \Delta_p^2\sigma_{p2} + \Delta_v\Delta_p\sigma_{vp} + O\left(\Delta_v^3, \Delta_p^3\right), \tag{3}$$

$$\begin{aligned} h(t) &= h_s + \frac{\Delta_v}{2}\left(h_{v11}e^{i\omega t} + h_{v12}e^{-i\omega t}\right) + \frac{\Delta_p}{2}\left(h_{p11}e^{i(\omega t-\delta)} + h_{p12}e^{-i(\omega t-\delta)}\right) \\ &+ \Delta_v\Delta_p\left(h_{vp} + h_{vp1}e^{i(2\omega t-\delta)} + h_{vp2}e^{-i(2\omega t-\delta)}\right) \\ &+ \Delta_v^2 h_{v2} + \Delta_p^2 h_{p2} + \frac{\Delta_v^2}{2}\left(h_{v31}e^{2i\omega t} + h_{v32}e^{-2i\omega t}\right) \\ &+ \frac{\Delta_p^2}{2}\left(h_{p31}e^{2i(\omega t-\delta)} + h_{p32}e^{-2i(\omega t-\delta)}\right) + O\left(\Delta_v^3, \Delta_p^3\right), \end{aligned} \tag{4}$$

$$\begin{aligned} w(z,t) &= w_s(z) + \frac{\Delta_v}{2}\left(w_{v11}(z)e^{i\omega t} + w_{v12}(z)e^{-i\omega t}\right) + \frac{\Delta_p}{2}\left(w_{p11}(z)e^{i(\omega t-\delta)}\right. \\ &+ \left. w_{p12}(z)e^{-i(\omega t-\delta)}\right) + \Delta_v^2 w_{v2}(z) + \Delta_p^2 w_{p2}(z) \\ &+ \Delta_v\Delta_p\left(w_{vp} + w_{vp1}e^{i(2\omega t-\delta)} + w_{vp2}e^{-i(2\omega t-\delta)}\right) \\ &+ \frac{\Delta_v^2}{2}\left(w_{v31}(z)e^{2i\omega t} + w_{v32}(z)e^{-2i\omega t}\right) + \frac{\Delta_p^2}{2}\left(w_{p31}(z)e^{2i(\omega t-\delta)}\right. \\ &+ \left. w_{p32}(z)e^{-2i(\omega t-\delta)}\right) + O\left(\Delta_v^3, \Delta_p^3\right). \end{aligned} \tag{5}$$

Note that the base flow $U(z,t)$ is an exact solution and does not rely on the smallness of Δ_v and Δ_p. After substituting the expansions (3-5) into the momentum equation (1) and interface conditions (2a-d), the partial differential system is reduced to a set of ordinary differential equations at $O\left(1, \Delta_v, \Delta_p, \Delta_v^2, \Delta_p^2, \Delta_v\Delta_p, \ldots\right)$. In the following section, these equations (given explicitly by A1-A6 in the Appendix) are discretized so that the eigenvalues σ can be obtained.

In the absence of imposed oscillations interfacial stability is determined by $\sigma = \sigma_s$. Our goal is to quantify the effect of the time-periodic forcing on the interfacial mode. The essential element of the above expansion scheme in small amplitudes $\Delta_v, \Delta_p \ll 1$ is that it becomes sufficient to solve for the steady component of the solution at $O\left(\Delta_v^2, \Delta_p^2, \Delta_v\Delta_p\right)$. This is due to the steady streaming effect where $O(\Delta_v, \Delta_p)$ perturbations interact with the base state. This differs from the longwave investigations (Yih 1968, Coward & Papageorgiou 1994) where the wavenumber is assumed small, but the amplitude of oscillations is not.

3 Numerical Solution

We discretize the vertical variation of $w(z,t)$ with a Chebyshev-tau scheme (Renardy & Renardy 1993) and denote the eigenproblem as

$$(\mathbf{A}-\sigma\mathbf{B})\,\mathbf{X}(t) \;=\; 0. \tag{6}$$

With $\Delta_v, \Delta_p \ll 1$ the eigenproblem (6) is expanded such that

$$\begin{aligned}\mathbf{X}(t) = \mathbf{X}_s &+ \frac{\Delta_v}{2}\left(\mathbf{X}_{v11}e^{i\omega t} + \mathbf{X}_{v12}e^{-i\omega t}\right) + \frac{\Delta_p}{2}\left(\mathbf{X}_{p11}e^{i(\omega t-\delta)} + \mathbf{X}_{p12}e^{-i(\omega t-\delta)}\right)\\ &+ \;\Delta_v^2\mathbf{X}_{v2} + \Delta_p^2\mathbf{X}_{p2} + \Delta_v\Delta_p\mathbf{X}_{vp} + \cdots.\end{aligned}$$

This small amplitude expansion enables us to reformulate the problem as a system of algebraic equations rather than a differential system in which time t appears explicitly. The expansion in the small amplitudes is crucial in achieving this simplifying effect. To leading order, $O(1)$, the eigenvalue σ_s is determined by solving $(\mathbf{A}_s-\sigma_s\mathbf{B})\,\mathbf{X}_s = 0$, which is the discretized form of the steady momentum equation and interface conditions (A1). At $O(\Delta_v)$ we have $(\mathbf{A}_s-\sigma_s\mathbf{B})\,\mathbf{X}_{v11} = -\mathbf{A}_v\mathbf{X}_s + i\omega\mathbf{B}\mathbf{X}_{v11}$ and $(\mathbf{A}_s-\sigma_s\mathbf{B})\,\mathbf{X}_{v12}=\overline{\mathbf{A}}_v\mathbf{X}_s - i\omega\mathbf{B}\mathbf{X}_{v12}$, which correspond to equations (A2). Note that $\overline{\mathbf{A}}_v$ is the complex conjugate of matrix $\mathbf{A}_v$. Similarly at $O(\Delta_p)$ we have $(\mathbf{A}_s-\sigma_s\mathbf{B})\,\mathbf{X}_{p11} = -\mathbf{A}_p\mathbf{X}_s + i\omega\mathbf{B}\mathbf{X}_{p11}$ and $(\mathbf{A}_s-\sigma_s\mathbf{B})\,\mathbf{X}_{p12} = \overline{\mathbf{A}}_p\mathbf{X}_s - i\omega\mathbf{B}\mathbf{X}_{p12}$. This is the discretized representation of equations (A3). Note that the expansion of σ contains no terms of $O(\Delta_v,\Delta_p)$. Such terms are found to be zero after substitution into the momentum equations and interface conditions. The higher order contributions to σ, namely σ_{v2}, σ_{p2} and σ_{vp} are obtained by solving the eigenrelations at $O\left(\Delta_v^2, \Delta_p^2, \Delta_v\Delta_p\right)$. These Floquet exponents are generated by the interaction between the $O(\Delta_v,\Delta_p)$ terms of the form $e^{i\omega t}, e^{-i\omega t}$ and the time dependent components of the base flow. The steady contributions at $O(\Delta_v^2)$, $O\left(\Delta_p^2\right)$ and $O(\Delta_v\Delta_p)$ respectively are

$$\begin{aligned}(\mathbf{A}_s-\sigma_s\mathbf{B})\,\mathbf{X}_{v2} &= \sigma_{v2}\mathbf{B}\mathbf{X}_s + \frac{1}{4}\left(\overline{\mathbf{A}}_v\mathbf{X}_{v11} - \mathbf{A}_v\mathbf{X}_{v12}\right),\\ (\mathbf{A}_s-\sigma_s\mathbf{B})\,\mathbf{X}_{p2} &= \sigma_{p2}\mathbf{B}\mathbf{X}_s + \frac{1}{4}\left(\overline{\mathbf{A}}_p\mathbf{X}_{p11} - \mathbf{A}_p\mathbf{X}_{p12}\right),\\ (\mathbf{A}_s-\sigma_s\mathbf{B})\,\mathbf{X}_{vp} &= \sigma_{vp}\mathbf{B}\mathbf{X}_s + \frac{1}{4}\left(\overline{\mathbf{A}}_v\mathbf{X}_{p11}e^{-i\delta} - \mathbf{A}_v\mathbf{X}_{p12}e^{i\delta}\right.\\ &\quad + \left.\overline{\mathbf{A}}_p\mathbf{X}_{v11}e^{i\delta} - \mathbf{A}_p\mathbf{X}_{v12}e^{-i\delta}\right).\end{aligned}$$

We define the adjoint system $\left(\overline{\mathbf{A}}_s^T - \overline{\sigma}_s \overline{\mathbf{B}}^T\right) \mathbf{Y}_s = 0$, so that the perturbed eigenvalues σ_{v2}, σ_{p2} and σ_{vp} are obtained by solving the adjoint conditions arising from the inner product $< \mathbf{Y}_s, (\mathbf{A} - \sigma \mathbf{B})\, \mathbf{X} >= 0$, where $\mathbf{X}$ is an arbitrary vector. $< \cdot, \cdot >$ denotes the following inner product (see Section 3 of Coward & Renardy 1996) of two functions g_1 and g_2, expanded in Chebyshev polynomials:

$$g_1 = \sum_{i=0}^{N} g_{1i} T_i(\tilde{z}) \exp(i\alpha_1 x), \qquad g_2 = \sum_{i=0}^{N} g_{2i} T_i(\tilde{z}) \exp(i\alpha_2 x),$$

$$(g_1, g_2) = \frac{\int_0^C \exp[i(-\alpha_1 + \alpha_2)x]\, dx}{\int_0^C dx} \times \sum_{i=0}^{N} \bar{g}_{1i} g_{2i}.$$

Here, $\tilde{z}$ is normalized to [-1,1] in the fluid layer, C represents a period in x, that is, a multiple of both $2\pi/\alpha_1$ and $2\pi/\alpha_2$. Thus, unless $-\alpha_1 + \alpha_2 = 0$, the inner product vanishes because of periodicity.

The eigenfunction Y_s to the adjoint problem has the same dependence on x as the eigenfunction. The normalization of $\mathbf{X}_s$ and $\mathbf{Y}_s$ is given by $< \mathbf{Y}_s, \mathbf{B}\mathbf{X}_s >= 1$. Therefore we obtain

$$< \mathbf{Y}_s, \left(\mathbf{A}_v \mathbf{X}_{v12} - \overline{\mathbf{A}}_v \mathbf{X}_{v11}\right) >= 4\sigma_{v2}, \quad < \mathbf{Y}_s, \left(\mathbf{A}_p \mathbf{X}_{p12} - \overline{\mathbf{A}}_p \mathbf{X}_{p11}\right) >= 4\sigma_{p2},$$
$$< \mathbf{Y}_s, \left(\mathbf{A}_v \mathbf{X}_{p12} e^{i\delta} - \overline{\mathbf{A}}_v \mathbf{X}_{p11} e^{-i\delta} + \mathbf{A}_p \mathbf{X}_{v12} e^{-i\delta} - \overline{\mathbf{A}}_p \mathbf{X}_{v11} e^{i\delta}\right) >= 4\sigma_{vp}.$$

We next consider two special cases for which we may derive closed form expressions for the growth rate of the interfacial mode: disturbances which have either asymptotically long or short wavelengths.

4 Asymptotic Analysis

4.1 Disturbances with Long Wavelengths

The growth rate for a steady flow is given by the real part of σ_s. The contribution due to boundary oscillations is σ_{v2}, while the oscillating pressure gradient gives rise to σ_{p2}. In addition, the stability is altered by the interaction of the oscillatory mechanisms, and is quantified by σ_{vp}. For the stability of steady two-layer flow to disturbances with wavelengths $\alpha \to 0$, the leading order growth rate Re $\sigma_s\,(m, r, R_1, l_1, G, F)$ is $O\,(\alpha^2)$. With flow parameters

$m = 10.1$, $r = 1$, $R_1 = 1$, $G = 0$, $T = 0$, $F^{-2} = 0$ and $l_1 = 2/7$ the asymptotic analysis yields Re $\sigma_s = 1.12637 \times \alpha^2$. Table 1 shows the computed results for Re σ_s based on the numerical scheme of the previous section. It also shows the generic dependence of Re σ_{v2}, Re σ_{p2}, and Re σ_{vp} on α^2. In the limit $\alpha \to 0$, Coward & Papageorgiou find that Re $\sigma_{v2} \equiv 4.70708 \times 10^{-4}\alpha^2$, when $\Delta = 0.01$. They denote the channel depth by L, the lower fluid depth by D, $a = L/D = 1/l_1$, and their Reynolds number is $ml_2\,(l + ml_2/l_1)\,R_1$. The agreement with Table 1 is evident.

α	$Re\ \sigma_s \times \alpha^{-2}$	$Re\ \sigma_{v2} \times \alpha^{-2}$	$Re\ \sigma_{p2} \times \alpha^{-2}$	$Re\ \sigma_{vp} \times \alpha^{-2}$
0.1	1.1102	4.0521×10^{-4}	5.4342×10^{-4}	-1.6634×10^{-3}
0.01	1.1261	4.6993×10^{-4}	5.6006×10^{-4}	-1.7626×10^{-3}

Table 1. Growth rates of disturbances to oscillatory plane Couette flow, as wavelength increases. $m = 10.1$, $l_1 = 2/7$, $R_1 = 1$, $G = 0$, $r = 1$, $T = 0$, $F^{-2} = 0$, $\omega = 1$ and $\delta = 0$.

Further information on the convergence of $\sigma_s + \Delta_v^2\sigma_{v2}$ for decreasing Δ_v is obtained by comparing our numerical calculations with the long wavelength asymptotic theory which is valid for all values of Δ_v. Table 2 illustrates some results based on the $\alpha \to 0$ analysis of Coward & Papageorgiou (1994). For this flow $\sigma_{v2} = 9.905 \times 10^{-11}$ with $\alpha = 0.001$. When Δ_v is small, this agrees with the second column of Table 2 which shows the component of the growth rate due to boundary oscillations for a given Δ_v and $\alpha \to 0$. For larger Δ_v, the results begin to diverge, higher order terms in Δ_v are playing a role here. The comparison between the overall growth rate for the longwave limit (column 3) and our numerical results is dominated by the magnitude of σ_s which is the same for both theories. As Δ_v becomes even larger, it is evident that our theory based on small amplitude of oscillation will no longer apply. However, even at $\Delta_v = 0.4$, we still see the same order of magnitude for σ_{v2} as the theory of Coward & Papageorgiou. This indicates that the trends we observe may persist to larger amplitudes. This motivates further work on finite amplitudes of oscillations, which is left for future study.

Δ_v	**Equivalent** $Re(\sigma_{v2})$ **with** $\alpha \to 0$	**Growth rate with** $\alpha \to 0$	$Re(\sigma = \sigma_s + \Delta_v^2 \sigma_{v2})$ **with** $\alpha = 0.001$
0.4	$2.2261 \times \alpha^2 \times 10^{-4}$	$7.4079 \times \alpha^2 \times 10^{-3}$	$7.3882 \times \alpha^2 \times 10^{-3}$
0.2	$1.6875 \times \alpha^2 \times 10^{-4}$	$7.3791 \times \alpha^2 \times 10^{-3}$	$7.3763 \times \alpha^2 \times 10^{-3}$
0.1	$1.3319 \times \alpha^2 \times 10^{-4}$	$7.3736 \times \alpha^2 \times 10^{-3}$	$7.3733 \times \alpha^2 \times 10^{-3}$
0.01	$1.0128 \times \alpha^2 \times 10^{-4}$	$7.3723 \times \alpha^2 \times 10^{-3}$	$7.3723 \times \alpha^2 \times 10^{-3}$

Table 2. Comparison of growth rates using long wavelength asymptotics (Coward & Papageorgiou 1994) and our numerical scheme for decreasing amplitude. $m = 2$, $l_1 = 2/7$, $R_1 = 1$, $G = 0$, $T = 0$, $F^{-2} = 0$, $r = 1$, $\omega = 1$ and $\delta = 0$.

4.2 Disturbances with Short Wavelengths

The short-wave asymptotics of the interfacial mode involves a boundary layer analysis locally around the interface. We rescale the z-coordinate (Hooper & Boyd 1983, Yiantsios & Higgins 1988a,b) and expand the variables in powers of $1/\alpha$ for $\alpha \gg 1$. We extend previous analyses to include not only the effect of a forcing pressure gradient but also time harmonic modulations of the upper boundary. To this end, we set $\eta = \alpha\,(z - l_1)$, $\eta = O\,(1)$ as $\alpha \to \infty$, and consider equations (1), (2a-d) when the streamwise wavelength is asymptotically large, $\alpha \gg 1$. We use the following expansions

$$
\begin{aligned}
w &= -i\alpha \left(\psi_0 + \frac{\psi_1}{\alpha} + \frac{\psi_2}{\alpha^2} + \frac{\psi_3}{\alpha^3} + \cdots \right) e^{-i\alpha f}, \\
h &= \alpha \left(h_0 + \frac{h_1}{\alpha} + \frac{h_2}{\alpha^2} + \frac{h_3}{\alpha^3} + \cdots \right) e^{-i\alpha f}, \\
\sigma &= -i\alpha c = -i\alpha U_s\,(z = l_1) - ic_0 - \frac{ic_1}{\alpha} - \frac{ic_2}{\alpha^2} - \frac{ic_3}{\alpha^3} + \cdots, \\
\frac{df}{dt} &= U\,(z = l_1, t) - U_s\,(z = l_1)\,,
\end{aligned}
$$

where $\psi_0, h_0, \psi_1, h_1, \ldots$ are periodic functions in t with period $2\pi/\omega$, and $c_0, c_1, \ldots$ are complex constants. We seek the first non-zero real contribution to σ to determine the temporal stability of the interface. The form of these expansions has been motivated by asymptotic analysis of the steady problem.

The no-slip boundary conditions are ψ , $\partial\psi/\partial\eta \to 0$ as $\eta \to \pm\infty$, and the leading order kinematic condition (2d) is

$$\frac{dh_0}{dt} = ic_0 h_0 \quad \Rightarrow \quad h_0 = h_{00} e^{ic_0 t},$$

which indicates that c_0 is an integer multiple of ω since $h_0(t)$ is periodic with period $2\pi/\omega$. To leading order, equations (1), (2a-d) yield the solution

$$\psi_0 = \begin{cases} a h_0 \eta e^{\eta} & \eta < 0, \\ -am h_0 \eta e^{-\eta} & \eta > 0, \end{cases} \qquad a(t) = \frac{(m-1)}{(m+1)} \frac{\partial U}{\partial z} \quad \text{at} \quad z = l_1^-.$$

To next order the kinematic condition is

$$\frac{dh_1}{dt} = ic_1 h_0 + ic_0 h_1 \quad \Rightarrow \quad h_1 = h_{10} e^{ic_0 t} + ic_1 t h_0.$$

Since $h_1(t)$ is periodic we require $c_1 = 0$. At $O(\alpha^{-1})$, the interface conditions (2a-d) and momentum equations (1) are essentially the same as their $O(1)$ counterparts since it is easily shown that as $\alpha \to \infty$,

$$U(z,t) - U(l_1,t) = \frac{\eta}{\alpha} \frac{\partial U}{\partial z}(l_1,t) + \frac{\eta^2}{2\alpha^2} \frac{\partial^2 U}{\partial z^2}(l_1,t) + O\left(\frac{1}{\alpha^3}\right).$$

The solution follows in the form

$$\psi_1 = \begin{cases} (a h_1 + b h_0)\, \eta e^{\eta} & \eta < 0, \\ (-ma h_1 + b h_0)\, \eta e^{-\eta} & \eta > 0, \end{cases} \qquad b(t) = \frac{m(1-r) R_1}{2r(m+1)} \frac{\partial U}{\partial t} \quad \text{at } z = l_1.$$

Continuing to next order we obtain momentum equations

$$\left(\frac{\partial^2}{\partial \eta^2} - 1\right)^2 \psi_2 = \begin{cases} 2R_1 h_0 e^{\eta} \left[ia\eta \frac{\partial U}{\partial z}\left(l_1^-, t\right) + \frac{da}{dt}\right] & \eta < 0, \\ 2mR_2 h_0 e^{-\eta} \left[ima\eta \frac{\partial U}{\partial z}\left(l_1^-, t\right) + \frac{da}{dt}\right] & \eta > 0. \end{cases}$$

These equations, together with the boundary conditions and the continuity of velocity at the interface (2a), yield the solution

$$\psi_2 = \begin{cases} (A + B_1 \eta) e^{\eta} + aE(\eta^3 - 3\eta^2) e^{\eta} + F_1 \eta^2 e^{\eta} & \eta < 0, \\ (A + B_2 \eta) e^{-\eta} + aEm^3 r^{-1} (\eta^3 + 3\eta^2) e^{-\eta} + m^2 r^{-1} F_1 \eta^2 e^{-\eta} & \eta > 0, \end{cases}$$

$$E = \frac{ih_0 R_1}{12} \left[\frac{1}{l_1} - \frac{l_1 G R_1}{2} + \left\{\left(d_v + d_p e^{-i\delta}\right) e^{i\omega t} + c.c.\right\}\right], \qquad F_1 = \frac{h_0 R_1}{4} \frac{da}{dt},$$

$$d_v = \frac{d_3\beta_1\Delta_v}{2}\cosh(\beta_1 l_1), \quad d_p = \frac{\beta_1\Delta_p}{2i\omega}\left[\sinh(\beta_1 l_1) + d_1\cosh(\beta_1 l_1)\right].$$

The kinematic condition determines the first imaginary component of the eigenvalue c, namely c_2, since

$$\frac{dh_2}{dt} = ic_0h_2 + ic_2h_0 - i\psi_2(0,t), \tag{7}$$

The continuity of normal stress at the interface (2c) determines A such that

$$\frac{(m+1)}{m}A = 6aE\left(\frac{m^2}{r}-1\right) - \frac{h_0R_1}{4}\frac{da}{dt}\left(1+\frac{m}{r}\right) - \frac{ih_0T\alpha^3}{2m} - \frac{i\alpha h_0R_1(r-1)}{2rF^2}.$$

B_1 and B_2 are not explicitly required here, but can easily be obtained from the equations of continuity of velocity and tangential stress (2a,2b). Finally then, we can determine c_2 which consists of the usual contribution from the steady flow, together with components which are also steady due to the interaction of oscillatory flow ($e^{i\omega t}$) and complex conjugates ($e^{-i\omega t}$),

$$\begin{aligned}
c_2 &= \frac{im\alpha R_1}{2(m+1)F^2}\left(\frac{1}{r}-1\right) - \frac{i\alpha^3T}{2(m+1)} + c_s + \Delta_v^2c_v + \Delta_p^2c_p + \Delta_v\Delta_pc_{vp},\\
c_s &= \frac{imR_1}{2}\frac{(1-m)}{(1+m)^2}\left[1-\frac{m^2}{r}\right]\left(\frac{1}{l_1}-\frac{GR_1l_1}{2}\right)^2,\\
c_v &= \frac{im\omega R_1^2}{4}\frac{(1-m)}{(1+m)^2}\left[1-\frac{m^2}{r}\right]|d_3\cosh(\beta_1 l_1)|^2,\\
c_p &= \frac{imR_1^2}{4\omega}\frac{(1-m)}{(1+m)^2}\left[1-\frac{m^2}{r}\right]|\sinh(\beta_1 l_1) + d_1\cosh(\beta_1 l_1)|^2,\\
c_{vp} &= \frac{imR_1^2(1-m)}{4(1+m)^2}\left[1-\frac{m^2}{r}\right]\left[d_3e^{i\delta}\cosh(\beta_1 l_1)\left(\overline{\sinh(\beta_1 l_1) + d_1\cosh(\beta_1 l_1)}\right)\right.\\
&\quad \left. + c.c.\right].
\end{aligned}$$

The leading order growth rates given above provide a useful check on the numerical scheme discussed in Section 2. For the case of plane Couette flow the numerical eigenvalue calculations give excellent agreement with c_s and c_v. In the presence of a non-zero pressure gradient the agreement is not as good. This discrepancy is explained by considering the $O(1/\alpha^3)$ contribution c_3. As shown below, this term is due entirely to the time dependence and quadratic

terms in the basic flow. For steady plane Couette flow $U_{zz} = 0$, $U_t = 0$ and it follows that c_3 is zero. Consequently, when $G = 0$ the shortwave expansion for the growth rate is in powers of α^{-2} as shown by the analysis of Hooper & Boyd (1983).

At $O(\alpha^{-3})$ the Orr-Sommerfeld equations (1) yield

$$\begin{aligned}
\left(D^2-1\right)^2\psi_3 &= \begin{cases} (A_1 + B_{11}\eta + C_1\eta^2)\, e^{\eta} & \eta < 0, \\ (A_2 + B_{21}\eta + C_2\eta^2)\, e^{-\eta} & \eta > 0, \end{cases} \\
A_1 &= 2R_1\left(h_1\frac{da}{dt} + h_0\frac{db}{dt}\right), \qquad A_2 = 2R_2\left(mh_1\frac{da}{dt} - h_0\frac{db}{dt}\right), \\
B_{11} &= 2iR_1\frac{\partial U_1}{\partial z}(l_1,t)\,[ah_1 + bh_0] - iah_0R_1\frac{\partial^2 U_1}{\partial z^2}(l_1,t), \\
B_{21} &= 2iR_2\frac{\partial U_2}{\partial z}(l_1,t)\,[amh_1 - bh_0] + iamh_0R_2\frac{\partial^2 U_2}{\partial z^2}(l_1,t), \\
C_1 &= iah_0R_1\frac{\partial^2 U_1}{\partial z^2}(l_1,t), \qquad C_2 = iamh_0R_2\frac{\partial^2 U}{\partial z^2}(l_1,t).
\end{aligned}$$

The solution follows in the form

$$\psi_3 = \begin{cases} (J + H_1\eta)\, e^{\eta} + \frac{1}{48}\left[(6A_1 - 6B_{11} + 9C_1)\,\eta^2 \right. \\ \qquad \left. + (2B_{11} - 4C_1)\,\eta^3 + C_1\eta^4\right] e^{\eta} & \eta < 0, \\ (J + H_2\eta)\, e^{-\eta} + \frac{1}{48}\left[(6A_2 + 6B_{21} + 9C_2)\,\eta^2 \right. \\ \qquad \left. + (2B_{21} + 4C_2)\,\eta^3 + C_2\eta^4\right] e^{-\eta} & \eta > 0. \end{cases}$$

H_1 and H_2 can be determined by the continuity of velocity and tangential stress at the interface. The kinematic condition is applied at $z = l_1$ and reads

$$\frac{dh_3}{dt} = ic_0h_3 + ic_1h_2 + ic_2h_1 + ic_3h_0 - iJ.$$

Clearly then c_3 is obtained through the imposition of the normal stress continuity. After some algebraic manipulations we obtain

$$\begin{aligned}
c_3 &= c_{s3} + \Delta_v^2 c_{v3} + \Delta_p^2 c_{p3} + \Delta_v\Delta_p c_{vp3}, \\
c_{s3} &= \frac{9imR_1^2G}{16}\frac{(1-m)}{(1+m)^2}\left(1 + \frac{m^2}{r}\right)\left(\frac{1}{l_1} - \frac{GR_1l_1}{2}\right), \\
c_{v3} &= \left[\frac{im^2R_1^2\,(r-1)}{16r\,(1+m)^2}\left(1 + \frac{m}{r}\right) + \frac{9imR_1^2\,(m-1)}{64\,(1+m)^2}\left(1 + \frac{m^2}{r^2}\right)\right]
\end{aligned}$$

$$\times \quad \left[\left\{i\omega U_v \overline{\frac{dU_v}{dz}}\right\} + c.c.\right],$$

$$c_{p3} = \frac{im^2R_1^2(r-1)}{16r(1+m)^2}\left(1+\frac{m}{r}\right)[\{i\omega U_p\} + c.c.]$$

$$+ \frac{9imR_1^2(m-1)}{64(1+m)^2}\left(1+\frac{m^2}{r^2}\right)\left[\left\{(i\omega U_p+1)\overline{\frac{dU_p}{dz}}\right\} + c.c.\right],$$

$$c_{vp3} = \frac{im^2R_1^2(r-1)}{16r(1+m)^2}\left(1+\frac{m}{r}\right)\left[\left\{i\omega e^{i\delta}U_v\overline{\frac{dU_p}{dz}} + i\omega e^{-i\delta}U_p\overline{\frac{dU_v}{dz}}\right\} + c.c.\right]$$

$$+ \frac{9imR_1^2(m-1)}{64(1+m)^2}\left(1+\frac{m^2}{r^2}\right)$$

$$\times \quad \left[\left\{i\omega e^{i\delta}U_v\overline{\frac{dU_p}{dz}} + \left(i\omega e^{-i\delta}U_p+1\right)\overline{\frac{dU_v}{dz}}\right\} + c.c.\right],$$

where the base flow and its derivatives (conjugates) are evaluated at $z = l_1$. Table 3 illustrates the results.

α	$Re(\sigma_s)\times\alpha^2$	$\mathbf{Re(\sigma_{v2})\times\alpha^2}$	$\mathbf{Re(\sigma_{p2})\times\alpha^2}$	$\mathbf{Re(\sigma_{vp})\times\alpha^2}$
5.0	0.0295	0.0150	0.0002	0.0004
10.0	0.0571	0.0304	0.0006	0.0095
20.0	0.0528	0.0298	0.0009	0.0105
50.0	0.0502	0.0297	0.0012	0.0118

Table 3. Oscillatory plane Couette-Poiseuille flow: Computed growth rates for disturbances with increasing wavenumber. $m = 0.5$, $l_1 = 0.7$, $R_1 = 1$, $G = 1.0$, $r = 1.0$, $T = 0$, $F^{-2} = 0$, $\omega = 1$ and $\delta = 0$.

The asymptotic results are:

$$Re\,\sigma_s = \frac{0.04847}{\alpha^2} + \frac{0.08426}{\alpha^3} + O\left(\frac{1}{\alpha^4}\right),\ Re\,\sigma_{v2} = \frac{0.02980}{\alpha^2} - \frac{0.00615}{\alpha^3} + O\left(\frac{1}{\alpha^4}\right),$$

$$Re\,\sigma_{p2} = \frac{0.00142}{\alpha^2} - \frac{0.01017}{\alpha^3} + O\left(\frac{1}{\alpha^4}\right),\ Re\,\sigma_{vp} = \frac{0.01275}{\alpha^2} - \frac{0.04559}{\alpha^3} + O\left(\frac{1}{\alpha^4}\right).$$

A comparison of the coefficients in the asymptotic expansions reveals that the correction terms in σ_s, σ_{p2} and σ_{vp} are necessary. For example, with $\alpha = 20$,

the asymptotics including the $O(\alpha^{-3})$ terms, agree with the numerical results up to the third significant figure: Re $\sigma_s \times \alpha^2 = 0.05268$, Re $\sigma_{v2} \times \alpha^2 = 0.02949$, Re $\sigma_{p2} \times \alpha^2 = 0.00091$, Re $\sigma_{vp} \times \alpha^2 = 0.01047$. With just the leading asymptotic term, the agreement is only to one significant figure.

5 Numerical Results

Before considering the stability of oscillating plane Couette-Poiseuille flow we study in detail the situation where the steady component of the pressure gradient is zero, $G = 0$, and the base flow is due to the motion of the upper boundary alone. The results have been convergence-tested.

5.1 The Couette Case: $G = 0$

In the absence of time-dependent forcing the base flow is steady two-layer plane Couette flow. The study of this flow is instructive in understanding of the phenomena which occur in more complicated flows. Here we quantify the effect of the oscillatory boundary motion and oscillatory pressure gradient on the interfacial mode.

The asymptotic expansion in powers of Δ_v and Δ_p begins with the leading order growth rate Re σ_s. If this is non-zero, then because the contributions from the modulations are quadratic in Δ_v and Δ_p, their effect is small. For a conclusion to be made, the critical case Re $\sigma_s = 0$ is considered. Then, stability is achieved when Re σ_{v2}, Re σ_{p2} and Re σ_{vp} combine to be negative. For illustrative purposes, we will show results at a chosen value of amplitude such as $\Delta_v = 0.2$; the trends observed there may persist for larger amplitudes but this needs to be verified with future work. In Figures 1(a-c) we consider the case when the lower fluid is more viscous than the one above ($m > 1$). The fluids have equal densities and the nondimensional coefficient of surface tension is $T = 0.001$, which has been included to stabilize short waves. As a sample low Reynolds number for the lower fluid, we choose $R_1 = 10$. Using a Newton-Raphson iteration scheme we then compute the critical wavenumbers and neutral stability curves which are illustrated in Figures 1(a) and 1(b) respectively. The dotted lines correspond to the unmodulated case $\Delta_v = \Delta_p = 0$ (Renardy 1989). The solid lines show the neutral stability curves when $\Delta_v = \Delta_p = 0.2$. The $-+-$ line shows results based on larger am-

plitude imposed oscillations, namely $\Delta_v = \Delta_p = 1.0$. Although our theory is based on small amplitude expansions, we include this extrapolated data to indicate the qualitative trends; quantitatively, the effect of larger amplitude forcing may in fact be more pronounced. Figure 1(c) gives a magnified view of the results shown in 1(b). On this graph we have also included the situation where there is no applied pressure gradient $\Delta_v = 0.2$ and $\Delta_p = 0$ (dashed line), and also the case without plate oscillations $\Delta_v = 0$ and $\Delta_p = 0.2$ (dashed/dotted line). For all $m > 1$ the time-periodic oscillations tend to increase the critical wavenumber. With a shallower more viscous lower fluid, the flow is destabilized by the interfacial mode. As the depth of the lower layer increases we cross the neutral curves depicted in 1(b,c), above which disturbances are stabilized by viscosity stratification. The imposition of the oscillatory forcing (by either or both mechanisms) has a destabilizing effect on the otherwise steady flow. The neutral curves are shifted to the left so that the region of instability is increased. When both boundary fluctuations and pressure gradient oscillations are present, and in-phase ($\delta = 0$), we see a noticeable increase in the critical wavenumber, especially for short wavelength disturbances. For $\alpha > 20$ the results illustrated in figures 1(a-c) are confirmed by the short wavelength asymptotic calculations.

The analysis of Coward & Papageorgiou (1994) assumes long wave perturbations but makes no assumptions on the size of the oscillation amplitude. These authors present evidence that an otherwise unstable flow can be stabilized by an oscillating upper boundary. For example, they show that for a more viscous and shallower upper fluid, the flow is stable when the oscillation amplitude exceeds 0.64 approximately (see their figures 4(b) and 5). Conversely, when the upper fluid is thin and less viscous than the fluid below, the flow is destabilized when the amplitude of the oscillations is approximately 0.57 or greater (see their figures 2(b) and 3). Our analysis, on the other hand, does assume small amplitudes, for which the effect on the growth rate is of quadratic order. Thus, the effects we show in the figures for $\Delta_v = \Delta_p = 0.2$ are numerically small, but the results are indicative of trends that may persist to larger values of the amplitudes (see the extrapolated $\Delta_v = \Delta_p = 1$ data in figure 1(a,b)). In particular, in viewing the interface height values on Figure 1(c) for $\Delta_v = \Delta_p = 0.2$, which vary approximately over 0.80 to 0.81 at the lower value of the viscosity ratio, these appear to be numerically close, but the complement of these, focusing on the thickness of the thinner layer, shows a 5 % difference. This shows that in terms of the layer thickness for a

thin lubricating layer, the results on differences in critical conditions can be significant. This effect would be even more pronounced at higher viscosity ratios.

We have also done extensive computations on the situation reverse to Figure 1, with a less viscous lower layer so that $m < 1$. In Figures 2(a,b) we illustrate our calculations of the critical wavenumbers and neutral stability curves for a representative flow with the lower fluid at low Reynolds number ($G = 0$, $R_1 = 10$, $\omega = 1$,$F^{-2} = 0$, $T = 0.001$, $\delta = 0$). We observe that with a viscosity ratio $0.13 < m < 0.39$ the combined effect of small amplitude oscillations in the pressure gradient and the boundary motion $\Delta_v = \Delta_p = 0.2$ (solid line) yield similar critical wavenumbers as the corresponding unmodulated case (dotted line). As m is increased above 0.4 approximately, the critical wavenumber is reduced by the imposition of time-periodic forcing. The effect of the oscillating boundary or pressure gradient alone however, leads to a slight increase in critical wavenumber over a significant range in viscosity ratio.

With a much more viscous upper fluid, the steady flow is unstable when interface height exceeds 0.251. With the inclusion of boundary and pressure oscillations of amplitudes $\Delta_v = 0.2 = \Delta_p$, instability is observed when $l_1 > 0.2482$, indicating a destabilizing effect on the flow. At a viscosity ratio of approximately $m = 0.23$ the neutral curves for the steady and the modulated flows coincide and a further increase in the viscosity ratio indicates that the periodic forcing has a small stabilizing role. The qualitative trends are indicated in Figures 2(a,b) by the extrapolated results with $\Delta_v = \Delta_p = 1$ (dashed line). Beyond $m \approx 0.51$ the critical wavenumber rapidly decreases and neutral stability points are given by the long wavelength theory.

Surface tension forces are parameterized by the non-dimensional group T and enter through the balance of normal stresses across the interface (see equation 2c). It is well known that for the unmodulated problem, surface tension stabilizes disturbances with short wavelengths, while it is of secondary importance to density and viscosity stratifications for long wavelength perturbations. We have observed similar trends in the presence of an oscillating boundary and/or time dependent pressure gradient. For moderate or large wavenumbers α the region of instability in $m - l_1$ parameter space is dramatically decreased as T increases. Additionally, critical wavenumbers are uniformly lowered (see figure 3 of Coward & Renardy 1996). For large α the numerical results rapidly approach those given by the leading terms in

the asymptotic analysis in Section 4. For neutral stability, the leading order critical wavenumber is determined by setting the real part of σ to zero:

$$\alpha = \left\{ \frac{mR_1\,(1-m)}{(1+m)\,T} \left(1 - \frac{m^2}{r}\right) \left[\left(\frac{1}{l_1} - \frac{GR_1 l_1}{2} \right)^2 + \frac{\omega R_1}{2} |\Delta_v d_3 \cosh\,(\beta_1 l_1)\,|^2 \right] \right\}^{\frac{1}{3}}.$$

Coward & Papageorgiou (1994) considered the effect of varying the frequency of the oscillations for long wavelength disturbances. They showed that increasing the frequency reduces the stabilizing or destabilizing effect of the unsteady terms. These results can be understood by considering the unperturbed flow at high oscillation frequencies. In such a regime the flow separates into a Stokes layer in the vicinity of the oscillating wall, and away from this layer the flow is almost steady and corresponds to two phase Couette flow due to a boundary which moves with constant velocity. As long as the Stokes layer is thin compared to the thickness of the upper layer, the interfacial mode is expected to be insensitive to the small amplitude wall modulations. The three graphs in Figures 3(a-c) extend these results for larger α. The solid lines plot the growth rate Re σ_{vp} against frequency $0.1 < \omega < 65$, while Re σ_{v2} and Re σ_{p2} are drawn with dashed lines and dashed/dotted lines. In Figure 3(a) we consider disturbances with long wavelengths $\alpha = 0.01$. The flow has a less viscous shallow lower layer. We find that as the frequency is increased, the growth rates of all three oscillatory components decrease. Thus at large frequencies $\omega > 50$ say, the stability characteristics of the oscillatory and steady flows are almost identical. With $\alpha = 1$ and 20 (Figures 3(b) and (c) respectively) this trend is again observed. For short waves, the destabilizing effect of the combined in-phase oscillations is suppressed by increasing the frequency ω. We note that although Re σ_{p2} is found to be an order of magnitude smaller than Re σ_{v2} and Re σ_{vp} this too decreases as ω is increased. We expect the large ω asymptotics to be a regular perturbation about the steady state; this may be analyzed by the method of averaging.

Finally, we analyze the role of the phase shift δ between the oscillatory pressure gradient and the planar motion of the upper boundary. The contribution to the growth rate by σ_{v2} and σ_{p2} arise due to the interactions of $e^{i(\omega t - \delta)}$ and their complex conjugates. Thus, the introduction of a phase shift $\delta \neq 0$ alters the stability of the flow through σ_{vp} alone. In Figures 4(a-d) we plot σ_s (dotted line), σ_{v2} (dashed line), σ_{p2} (dashed/dotted line) and σ_{vp}

(solid line) against $0 < \delta < 2\pi$ for a variety of flows. In
that by altering the phase shift, the oscillatory forcing can e
destabilize the flow. These figures show regimes where the
σ_{vp} has an opposite sign to σ_{v2}, σ_{p2} and σ_s, so that the total
posite from a simple comparison of the separate effects of mo
or pressure gradient independently. The magnitude of δ req
maximum stabilization or destabilization depends upon th
parameters of the flow. The values of δ for the two situati
as evident in Figure 4(d) which shows plane Couette flow w
viscous lower fluid. The perturbations to the flow have wave
When the boundary and pressure fluctuations are in-phase,
At $\delta \approx \pi/2$ maximum stability is obtained. Conversely a
destabilizing role of σ_{vp} is at its greatest. Thus the combine
lating the wall and the pressure gradient is not simply the
their separate effects.

5.2 The Poiseuille Case: $U_u^* = 0$

When the mean upper boundary is stationary, the base flo
two-layer plane Poiseuille flow. One difference with the Coue
the second derivative of the base flow enters into the correcti
short-wave asymptotic formulas, necessitating the inclusion
terms. This shifts the critical wavenumbers in the short-w
the formula given in Section 4. In Figures 5(a,b) we consi
stability curves of oscillatory plane Poiseuille flow with a mor
fluid layer ($R_1 = 10$, $T = 0.1$); (a) shows critical wavenumbers
the minimum interface height for which instability is possible.
pressure gradient G is determined by the steady base flow at
such that $G = 2\,(l_1 + ml_2)\,/\,(ml_1 l_2 R_1)$. The oscillations of
and pressure gradient are in-phase ($\delta = 0$) and have frequen
Figures 5(a,b) the solid lines show the effect of the combined os
with amplitude 0.2, while in the absence of periodic forcing w
stability and critical wavenumbers plotted by the dotted line.
effects with $\Delta_v = 0.2$, $\Delta_p = 0$ and $\Delta_v = 0$, $\Delta_p = 0.2$ are given
and dashed/dotted lines respectively. In the region below the
in 5(b), the flow is linearly stable. As evident, for $m > 1$, insta
possible when the upper fluid is relatively thin. These figures s

region of instability is increased by the modulations. In Table 4 we quantify the position of the minimum value of the interface heights for instability, and show the uniformly destabilizing effect of the oscillatory forcing for this flow. The critical wavenumbers (Figure 5(a)) can move either way.

Amplitude Δ_v	**Amplitude** Δ_p	**Viscosity Ratio** m	**Min. Int. Height** l_1	**Critical Wavenum.** α_c
0	0	5.220	0.74489	6.095
0.2	0	5.194	0.74368	6.076
0	0.2	5.192	0.74487	6.111
0.2	0.2	5.131	0.74238	6.096

Table 4. Oscillatory plane Poiseuille flow: Minimum interface heights below which all disturbances are stable. ($U_u^* = 0, R_1 = 10, G \neq 0, r = 1.0, F^{-2} = 0, \omega = 1, \delta = 0$).

In addition to changing the neutral stability, the imposed oscillations also alter the critical wavenumbers plotted in Figure 5(a). For $m < 4.8$ (approximately) the critical wavenumbers are decreased by the imposition of an oscillatory boundary and/or pressure gradient. For larger values of viscosity ratio we see a marked reduction in the critical α for all three cases involving the time-periodic forcing.

5.3 The Couette-Poiseuille Case

We now consider a flow where both the upper boundary and the pressure gradient have a constant component and a time-periodic contribution. When the lower fluid is thin and less viscous, the unmodulated flow is found to be unstable for a wide parameter range. The oscillatory boundary motion with small amplitude Δ_v can have a stabilizing effect however. In Figure 6(a) we plot the growth rate Re σ against viscosity ratio m for a plane Couette-Poiseuille flow with parameters: $R_1 = 1$, $l_1 = 0.34$, $\alpha = 1$, $G = 18$, $\omega = 1$, $T = 0.003$ and $r = 4$. The dotted line corresponds to the growth rate Re σ_s of the unmodulated flow and the solid line demonstrates the stabilizing effect of the oscillatory motion of the upper plate with magnitude $\Delta_v = 0.2$. We note that for a significant range in viscosity ratio the otherwise linearly unstable

flow is completely stabilized by the imposed oscillations. contributions to σ due to the pressure fluctuations (namely in fact negligible for this particular flow.

In Figure 6(b) we illustrate the effect of the forced oscill which has a deeper, less viscous lower layer. For viscosity r $m < 1$ the growth rates σ_{v2}, σ_{p2} and σ_{vp} are positive ar oscillatory motion has a destabilizing influence. As in the the dotted line is for the unmodulated flow (Re σ_s) while the complete growth rate Re σ.

In Figure 7, we display Re σ_s, Re σ_{v2}, Re σ_{p2} and Re σ_{vp} ag ber α, for different layer depths. The broken lines correspon equal depths, the solid line is for a deeper lower fluid, $l_1 = 0.6$, line is for a shallower lower layer with $l_1 = 0.4$. There is a com ior of the curves from each of the terms. At each wavenumbe of these contributions determines the stability. Finally, the of density stratification on the stability is shown in Figure 9(l Renardy.

6 Conclusions

We have considered the effect of time harmonic modulations t velocity and pressure gradient which drive the flow of two flui parallel plates. Our main aim is to demonstrate that such m have a stabilizing or destabilizing effect on the interfacial mo

The base flow is in the streamwise direction and has a s nent and time-periodic part. The perturbations to the flow ha wavenumber α. With $\alpha \gg 1$ we present an asymptotic analysi a closed form expression for the growth rate accurate to $O(\alpha^-$ plane Couette flow, the $O(\alpha^{-3})$ term vanishes but the time de quadratic profile in the base flow may generate significant coefl order. For long wavelength disturbances to the oscillatory flo ical results generalize the asymptotic results on Couette flow Coward & Papageorgiou (1994).

We have considered separately plane Couette, plane Poiseu bined Couette-Poiseuille flows. The imposed oscillations are ass small amplitudes and this simplifies the analysis for the quadrat

correct the unmodulated interfacial eigenvalue. Being quadratic in the amplitudes, these are numerically small effects, but are expected to show trends that persist to larger amplitudes. Such trends need to be verified with future work on finite amplitudes of oscillations. We have taken sample situations at low Reynolds numbers for the lower liquid and $\Delta_v, \Delta_p = 0.2$, and focussed on the viscosity stratification. For the critical cases we examined, we have $Re\ \sigma_{v2}$ and $Re\ \sigma_{vp}$ larger than $Re\ \sigma_{p2}$. With the assumption of small oscillations, we are able to demonstrate *complete* stabilization or destabilization of the interface by in cases where the otherwise unmodulated interfacial mode has a growth rate Re σ_s which is small.

The combined stabilizing/destabilizing effect of boundary and pressure oscillations (σ_{vp}) cannot be inferred from the separate contributions to the growth rate, namely σ_{v2} and σ_{p2}. We have presented examples where Re σ_{v2}, Re $\sigma_{p2} > 0$ whereas the combined effect stabilizes the interfacial mode. Moreover, the phase shift δ can alter the magnitude and sign of Re σ_{vp}.

7 Acknowledgements

This work is supported by the National Science Foundation under Grant No. CTS-9307238 and the Office of Naval Research under grant No. N00014-92-J-1664. Y. R. acknowledges the hospitality of the Institute for Mathematics and Its Applications (Minnesota) and the Isaac Newton Institute for Mathematical Sciences (Cambridge).

Appendix: Small Amplitude Expansion

With $\Delta_v, \Delta_p \ll 1$, the eigenvalue σ, interface height $h(t)$ and velocity $w(t)$ are expanded asymptotically according to equations (3-5). The momentum equations (1) and interface conditions (2a-2d) yield the systems of steady equations listed below. Using the notation $[\![x]\!] \equiv x$(fluid 1) - x(fluid 2), evaluated at $z = l_1$, the leading order steady equations are

$$\frac{1}{R_i}\left(\frac{d^4}{dz^4} - 2\alpha^2\frac{d^2}{dz^2} + \alpha^4\right) w_s = (i\alpha U_s + \sigma_s)\left(\frac{d^2}{dz^2} - \alpha^2\right) w_s - i\alpha w_s \frac{d^2 U_s}{dz^2}, \quad \text{(A1)}$$

$$[\![w_s]\!] = 0, \quad \sigma_s h_s + i\alpha h_s U_s - w_s = 0, \quad \text{at} \quad z = l_1,$$

$$i\alpha h_s\left(1-m\right)\left[\frac{1}{l_1}-\frac{GR_1l_1}{2}\right]-[\![\frac{dw_s}{dz}]\!]=0,\quad [\![\frac{\mu}{\mu_1}\left(\frac{d^2w_s}{dz^2}+\right.$$ 0,

$$[\![\frac{\mu}{\mu_1R_1}\left(3\alpha^2\frac{dw_s}{dz}-\frac{d^3w_s}{dz^3}\right)]\!]+\frac{\alpha^4h_sT}{mR_1}+\frac{h_s}{}$$ +

$$[\![\frac{\rho}{\rho_1}\left(\sigma_s\frac{dw_s}{dz}-i\alpha w_s\frac{dU_s}{dz}+i\alpha U_{s}\right.$$ 0.

At $O\left(\Delta_v\right)$ the system is

$$\frac{1}{R_i}\left(\frac{d^4}{dz^4}-2\alpha^2\frac{d^2}{dz^2}+\alpha^4\right)w_{v11}-i\alpha U_s\left(\frac{d^2}{dz^2}-\alpha^2\right)w_{v11}+$$ $\frac{U_s}{2}$

$$-i\alpha U_v\left(\frac{d^2}{dz^2}-\alpha^2\right)w_s+i\alpha w_s\frac{d^2U_v}{dz^2}=\left(\sigma_s+i\omega\right)\left(\frac{d^2}{dz^2}-\right.$$ (A2)

$$[\![w_{v11}]\!]=0,\quad \left(\sigma_s+i\omega\right)h_{v11}+i\alpha h_{v11}U_s+i\alpha h_sU_v-w_{v11}=0$$,

$$i\alpha h_s[\![\frac{dU_v}{dz}]\!]+i\alpha h_{v11}\left(1-m\right)\left[\frac{1}{l_1}-\frac{GR_1l_1}{2}\right]-[\![$$,

$$\alpha\omega h_sR_1\frac{\left(r-1\right)}{r}U_v+[\![\frac{\mu}{\mu_1}\left(\frac{d^2w_{v11}}{dz^2}+\alpha^2u\right.$$,

$$[\![\frac{\mu}{\mu_1R_1}\left(3\alpha^2\frac{dw_{v11}}{dz}-\frac{d^3w_{v11}}{dz^3}\right)]\!]+\frac{\alpha^4h_{v11}T}{mR_1}+\frac{h_{v11}\alpha^2}{r}$$

$$[\![\frac{\rho}{\rho_1}\left(\left(\sigma_s+i\omega\right)\frac{dw_{v11}}{dz}-i\alpha w_{v11}\frac{dU_s}{dz}+i\alpha U_s\frac{du}{d}\right.$$

At $O\left(\Delta_p\right)$ we have

$$\frac{1}{R_i}\left(\frac{d^4}{dz^4}-2\alpha^2\frac{d^2}{dz^2}+\alpha^4\right)w_{p11}-i\alpha U_s\left(\frac{d^2}{dz^2}-\alpha^2\right)w_{p11}+i\alpha$$

$$-i\alpha U_p\left(\frac{d^2}{dz^2}-\alpha^2\right)w_s+i\alpha w_s\frac{d^2U_p}{dz^2}=\left(\sigma_s+i\omega\right)\left(\frac{d^2}{dz^2}-\alpha^{2}\right.$$ 3)

$$[\![w_{p11}]\!]=0,\quad \left(\sigma_s+i\omega\right)h_{p11}+i\alpha h_{p11}U_s+i\alpha h_sU_p-w_{p11}=0,\ a$$

$$i\alpha h_s[\![\frac{dU_p}{dz}]\!]+i\alpha h_{p11}\left(1-m\right)\left[\frac{1}{l_1}-\frac{GR_1l_1}{2}\right]-[\![\frac{du}{d}$$

$$\alpha\omega h_sR_1\frac{\left(r-1\right)}{r}U_p+[\![\frac{\mu}{\mu_1}\left(\frac{d^2w_{p11}}{dz^2}+\alpha^2w_{p}\right.$$

$$[\![\frac{\mu}{\mu_1 R_1}\left(3\alpha^2\frac{dw_{p11}}{dz}-\frac{d^3w_{p11}}{dz^3}\right)]\!]+\frac{\alpha^4 h_{p11}T}{mR_1}+\frac{h_{p11}\alpha^2(r-1)}{rF^2}+$$
$$[\![\frac{\rho}{\rho_1}\left((\sigma_s+i\omega)\frac{dw_{p11}}{dz}-i\alpha w_{p11}\frac{dU_s}{dz}+i\alpha U_s\frac{dw_{p11}}{dz}\right)]\!]=0.$$

The steady system of equations at $O\left(\Delta_v^2\right)$ is

$$\frac{1}{R_i}\left(\frac{d^4}{dz^4}-2\alpha^2\frac{d^2}{dz^2}+\alpha^4\right)w_{v2}-i\alpha U_s\left(\frac{d^2}{dz^2}-\alpha^2\right)w_{v2}+i\alpha w_{v2}\frac{d^2U_s}{dz^2}-$$
$$\frac{i\alpha}{4}\left[\overline{U}_v\left(\frac{d^2}{dz^2}-\alpha^2\right)w_{v11}+U_v\left(\frac{d^2}{dz^2}-\alpha^2\right)w_{v12}-w_{v11}\frac{d^2\overline{U}_v}{dz^2}-w_{v12}\frac{d^2U_v}{dz^2}\right]$$
$$=\left(\frac{d^2}{dz^2}-\alpha^2\right)\left(\sigma_s w_{v2}+\sigma_{v2}w_s\right), \quad \text{(A4)}$$

$$\sigma_s h_{v2}+\sigma_{v2}h_s+\frac{i\alpha}{4}\left[h_{v11}\overline{U}_v+h_{v12}U_v\right]+i\alpha h_{v2}U_s-w_{v2}=0, \quad \text{at} \quad z=l_1,$$

$$\frac{i\alpha}{4}\left[h_{v12}[\![\frac{dU_v}{dz}]\!]+h_{v11}[\![\frac{d\overline{U}_v}{dz}]\!]\right]+i\alpha h_{v2}(1-m)\left[\frac{1}{l_1}-\frac{GR_1l_1}{2}\right]-[\![\frac{dw_{v2}}{dz}]\!]=0,$$

$$[\![\frac{\mu}{\mu_1}\left(\frac{d^2w_{v2}}{dz^2}+\alpha^2w_{v2}-\frac{i\alpha}{4}\left[h_{v11}\frac{d^2\overline{U}_v}{dz^2}+h_{v12}\frac{d^2U_v}{dz^2}\right]\right)]\!]=0,$$

$$[\![w_{v2}]\!]=0, \quad [\![\frac{\mu}{\mu_1 R_1}\left(3\alpha^2\frac{dw_{v2}}{dz}-\frac{d^3w_{v2}}{dz^3}\right)]\!]+\frac{\alpha^4h_{v2}T}{mR_1}+\frac{h_{v2}\alpha^2(r-1)}{rF^2}+$$
$$[\![\frac{\rho}{\rho_1}\left(\sigma_s\frac{dw_{v2}}{dz}+\sigma_{v2}\frac{dw_s}{dz}-i\alpha w_{v2}\frac{dU_s}{dz}-\frac{i\alpha}{4}\left[w_{v12}\frac{dU_v}{dz}+w_{v11}\frac{d\overline{U}_v}{dz}\right]+\right.$$
$$\left.i\alpha U_s\frac{dw_{v2}}{dz}+\frac{i\alpha}{4}\left[U_v\frac{dw_{v12}}{dz}+\overline{U}_v\frac{dw_{v11}}{dz}\right]\right)]\!]=0.$$

The steady contribution at $O\left(\Delta_p^2\right)$ is

$$\frac{1}{R_i}\left(\frac{d^4}{dz^4}-2\alpha^2\frac{d^2}{dz^2}+\alpha^4\right)w_{p2}-i\alpha U_s\left(\frac{d^2}{dz^2}-\alpha^2\right)w_{p2}+i\alpha w_{p2}\frac{d^2U_s}{dz^2}-$$
$$\frac{i\alpha}{4}\left[\overline{U}_p\left(\frac{d^2}{dz^2}-\alpha^2\right)w_{p11}+U_p\left(\frac{d^2}{dz^2}-\alpha^2\right)w_{p12}-w_{p11}\frac{d^2\overline{U}_p}{dz^2}-w_{p12}\frac{d^2U_p}{dz^2}\right]$$
$$=\left(\frac{d^2}{dz^2}-\alpha^2\right)\left(\sigma_s w_{p2}+\sigma_{p2}w_s\right), \quad \text{(A5)}$$

$$\sigma_s h_{p2} + \sigma_{p2} h_s + \frac{i\alpha}{4}\left[h_{p11}\overline{U}_p + h_{p12}U_p\right] + i\alpha h_{p2}U_s - w_{p2} = 0, \quad \text{at} \quad z = l_1,$$

$$\frac{i\alpha}{4}\left[h_{p12}[\![\frac{dU_p}{dz}]\!] + h_{p11}[\![\frac{d\overline{U}_p}{dz}]\!]\right] + i\alpha h_{p2}(1-m)\left[\frac{1}{l_1} - \frac{GR_1 l_1}{2}\right] - [\![\frac{dw_{p2}}{dz}]\!] = 0,$$

$$[\![w_{p2}]\!] = 0, \quad [\![\frac{\mu}{\mu_1}\left(\frac{d^2 w_{p2}}{dz^2} + \alpha^2 w_{p2} - \frac{i\alpha}{4}\left[h_{p11}\frac{d^2\overline{U}_p}{dz^2} + h_{p12}\frac{d^2 U_p}{dz^2}\right]\right)]\!] = 0,$$

$$[\![\frac{\mu}{\mu_1 R_1}\left(3\alpha^2\frac{dw_{p2}}{dz} - \frac{d^3 w_{p2}}{dz^3}\right)]\!] + \frac{\alpha^4 h_{p2} T}{mR_1} + \frac{h_{p2}\alpha^2(r-1)}{rF^2} +$$

$$[\![\frac{\rho}{\rho_1}\left(\sigma_s\frac{dw_{p2}}{dz} + \sigma_{p2}\frac{dw_s}{dz} - i\alpha w_{p2}\frac{dU_s}{dz} - \frac{i\alpha}{4}\left[w_{p12}\frac{dU_p}{dz} + w_{p11}\frac{d\overline{U}_p}{dz}\right] +\right.$$

$$\left. i\alpha U_s\frac{dw_{p2}}{dz} + \frac{i\alpha}{4}\left[U_p\frac{dw_{p12}}{dz} + \overline{U}_p\frac{dw_{p11}}{dz}\right]\right)]\!] = 0.$$

The steady contribution at $O(\Delta_v\Delta_p)$ is

$$\frac{1}{R_i}\left(\frac{d^4}{dz^4} - 2\alpha^2\frac{d^2}{dz^2} + \alpha^4\right)w_{vp} - i\alpha U_s\left(\frac{d^2}{dz^2} - \alpha^2\right)w_{vp} + i\alpha w_{vp}\frac{d^2 U_s}{dz^2}$$

$$-\frac{i\alpha e^{i\delta}}{4}\left[\overline{U}_p\left(\frac{d^2}{dz^2} - \alpha^2\right)w_{v11} + U_v\left(\frac{d^2}{dz^2} - \alpha^2\right)w_{p12}\right]$$

$$-\frac{i\alpha e^{-i\delta}}{4}\left[\overline{U}_v\left(\frac{d^2}{dz^2} - \alpha^2\right)w_{p11} + U_p\left(\frac{d^2}{dz^2} - \alpha^2\right)w_{v12}\right]$$

$$+\frac{i\alpha e^{i\delta}}{4}\left[w_{v11}\frac{d^2\overline{U}_p}{dz^2} + w_{p12}\frac{d^2 U_v}{dz^2}\right] + \frac{i\alpha e^{-i\delta}}{4}\left[w_{p11}\frac{d^2\overline{U}_v}{dz^2} + w_{v12}\frac{d^2 U_p}{dz^2}\right]$$

$$= \left(\frac{d^2}{dz^2} - \alpha^2\right)(\sigma_s w_{vp} + \sigma_{vp} w_s), \qquad \text{(A6)}$$

$$\frac{i\alpha}{4}\left[h_{p11}\overline{U}_v e^{-i\delta} + h_{v11}\overline{U}_p e^{i\delta} + h_{v12}U_p e^{-i\delta} + h_{p12}U_v e^{i\delta}\right]$$

$$+\sigma_s h_{vp} + \sigma_{vp} h_s + i\alpha h_{vp} U_s - w_{vp} = 0, \quad \text{at} \quad z = l_1,$$

$$\frac{i\alpha e^{i\delta}}{4}\left[h_{p12}[\![\frac{dU_v}{dz}]\!] + h_{v11}[\![\frac{d\overline{U}_p}{dz}]\!]\right] + \frac{i\alpha e^{-i\delta}}{4}\left[h_{v12}[\![\frac{dU_p}{dz}]\!] +\right.$$

$$\left. h_{p11}[\![\frac{d\overline{U}_v}{dz}]\!]\right] + i\alpha h_{vp}(1-m)\left[\frac{1}{l_1} - \frac{GR_1 l_1}{2}\right] - [\![\frac{dw_{vp}}{dz}]\!] = 0,$$

$$[\![w_{vp}]\!] = 0, \qquad [\![\frac{\mu}{\mu_1}\left(\frac{d^2 w_{vp}}{dz^2} + \alpha^2 w_{vp} - \frac{i\alpha e^{i\delta}}{4}\left[h_{p12}\frac{d^2 U_v}{dz^2} + h_{v11}\frac{d^2\overline{U}_p}{dz^2}\right]\right.$$

$$-\frac{i\alpha e^{-i\delta}}{4}\left[h_{p11}\frac{d^2\overline{U}_v}{dz^2}+h_{v12}\frac{d^2U_p}{dz^2}\right]\Big)\Big]=0,$$

$$\Big[\frac{\mu}{\mu_1 R_1}\left(3\alpha^2\frac{dw_{vp}}{dz}-\frac{d^3w_{vp}}{dz^3}\right)\Big]+\frac{\alpha^4 h_{vp}T}{mR_1}+\frac{h_{vp}\alpha^2\left(r-1\right)}{rF^2}+$$

$$\Big[\frac{\rho}{\rho_1}\left(\sigma_s\frac{dw_{vp}}{dz}+\sigma_{vp}\frac{dw_s}{dz}-i\alpha w_{vp}\frac{dU_s}{dz}+i\alpha U_s\frac{dw_{vp}}{dz}+\right.$$

$$\frac{i\alpha e^{i\delta}}{4}\left[U_v\frac{dw_{p12}}{dz}+\overline{U}_p\frac{dw_{v11}}{dz}-w_{p12}\frac{dU_v}{dz}-w_{v11}\frac{d\overline{U}_p}{dz}\right]+$$

$$\left.\frac{i\alpha e^{-i\delta}}{4}\left[\overline{U}_v\frac{dw_{p11}}{dz}+U_p\frac{dw_{v12}}{dz}-w_{p11}\frac{d\overline{U}_v}{dz}-w_{v12}\frac{dU_p}{dz}\right]\right)\Big]=0.$$

References

Aminataei, A., Maithili Sharan & Singh, M.P. 1988 Two-layer model for the process of blood oxygenation in the pulmonary capillaries: parabolic profiles in the core as well as in the plasma layer. *Appl. Math. Modelling*, **12**, pp. 601-609.

Chen, Y. & Aidun, C. 1994 An inviscid mode of instability in a two-layer inclined channel flow. *Bull. Amer. Phys. Soc.*, **39**(9), pp. 1933.

Coward, A.V. & Papageorgiou, D.P. 1994 Stability of oscillatory two-phase Couette flow. *IMA J. Appl. Math.*, **53**, pp. 75-93.

Coward, A.V., Papageorgiou, D.P. & Smyrlis, Y.S. 1995 Nonlinear stability of oscillatory core-annular flow: a generalized Kuramoto-Sivashinsky equation with time-periodic coefficients. *Z. angew. Math Phys.*, **46**, pp. 1-39.

Coward, A.V. & Renardy, Y.Y. 1996 Small amplitude oscillatory forcing on two-layer plane channel flow. Interdisciplinary Center for Applied Mathematics Report, V. P. I. & S. U.

Davis, S.H. 1976 The stability of time-periodic flows. *Ann. Rev. Fluid Mech.*, **8**, pp. 57-74.

Grosch, C. E. & Salwen, H. 1968 The stability of steady and time-dependent plane Poiseuille flow. *J. Fluid Mech.*, **34**, pp. 177-205.

Hall, P. 1975 The stability of Poiseuille flow modulated at high frequencies. *Proc. R. Soc. Lond.*, A**344**, pp. 453-464.

Hinch, E.J. 1984 A note on the mechanism of the instability at the interface between two shearing fluids. *J. Fluid Mech.*, **144**, pp. 463-468.

Hooper, A.P. 1985 Long-wave instability at the interface between two viscous fluids: Thin layer effects. *Phys. Fluids*, **28**(6), pp. 1613-1618.

Hooper, A.P. & Boyd, W.G.C. 1983 Shear-flow instability at the interface between two viscous fluids. *J. Fluid Mech.*, **128**, pp. 507-528.

Hu, H.-C.& Kelly, R.E. 1995 Stabilization of Taylor vortices by means of a time-periodic axial shear flow: non-axisymmetric disturbances. *Phys Rev. E*, **51**, pp. 3242-3251.

Joseph, D.D. & Renardy, Y. 1993 Fundamentals of two-fluid dynamics. Vol. 1 & 2 *Springer-Verlag, New York.*

Kelly, R.E. & Hu, H.-C. 1993 The onset of Rayleigh-Benard convection in non-planar oscillatory flows. *J. Fluid Mech.*, **249**, pp. 373-390.

Ranjbaran, M.M. & Khomami, B. 1996 The effect of interfacial instabilities on the strength of the interface in two-layer plastic structures. *Polym. Eng. Sci. In the press.*

Renardy, M. & Renardy, Y.Y. 1993 Derivation of amplitude equations and the analysis of sideband instabilities in two-layer flows. *Phys. Fluids*, **A5**(11), pp. 2738-2762, ibid, **A6**(10) pp. 3502.

Renardy, Y.Y. 1985 Instability at the interface between two shearing fluids in a channel. *Phys. Fluids*, **28**, pp. 3441-3443.

Renardy, Y.Y. 1987 The thin-layer effect and interfacial stability in a two-

layer Couette flow with similar liquids. *Phys. Fluids*, **30**(6), pp.1627-1637.

Renardy, Y.Y. 1995 Weakly nonlinear behavior of periodic disturbances in two-layer plane channel flow of upper-convected Maxwell liquids. *J. Non-Newtonian Fluid Mech.*, **56**, pp. 101-126.

Tilley, B.S., Davis, S.H. & Bankoff, S.G. 1994a Nonlinear long-wave stability of superposed fluids in an inclined channel. *J. Fluid Mech.*, **277**, pp. 58-83.

Tilley, B.S., Davis, S.H. & Bankoff, S.G. 1994b Linear stability theory of two-layer fluid flow in an inclined channel. *Phys. Fluids*, **6**, pp. 3906-3922.

von Kerczek, C. H. 1982 Instability of oscillatory plane Poiseuille flow. *J. Fluid Mech.*, **116**, pp. 91-114.

von Kerczek, C. H. 1987 Stability characteristics of oscillatory flows: Poiseuille, Ekman and films. In Stability of Time Dependent and Spatially Varying Flows. *D.L. Dwoyer & M.Y. Hussaini, eds, Springer-Verlag.*

Yiantsios, S.G. & Higgins, B.G. 1988a Numerical solution of eigenvalue problems using the compound matrix method. *J. Comput. Phys.*, **74** pp. 25-40.

Yiantsios, S.G. & Higgins, B.G. 1988b Linear stability of plane Poiseuille flow of two superposed fluids. *Phys. Fluids*, **31**, pp. 3225-3238.

Yih, C.-S. 1967 Instability due to viscosity stratification. *J. Fluid Mech.*, **27**, pp. 337-352.

Yih, C.-S. 1968 Instability of unsteady flows or configurations Part 1. Instability of a horizontal liquid layer on an oscillating plate. *J. Fluid Mech.*, **31**, pp. 737-751.

Figure Captions

Figure 1(a). Critical wavenumbers for plane Couette flow with a more viscous lower fluid. $\Delta_v = \Delta_p = 0$ (dotted line), $\Delta_v = \Delta_p = 0.2$ (solid line), $\Delta_v = \Delta_p = 1$ (–+– line). $r = 1$, $R_1 = 10$, $m > 1$, $G = 0$, $\omega = 1$, $T = 0.001$, $F^{-2} = 0$ and $\delta = 0$.

Figure 1(b). Neutral stability curves for plane Couette flow with a more viscous lower fluid. $\Delta_v = \Delta_p = 0$ (dotted line), $\Delta_v = \Delta_p = 0.2$ (solid line), $\Delta_v = \Delta_p = 1$ (+ line). Physical parameters are the same as in figure 1(a).

Figure 1(c). Expanded view of the neutral stability curves in figure 1(b). $\Delta_v = \Delta_p = 0$ (dotted line), $\Delta_v = \Delta_p = 0.2$ (solid line), $\Delta_v = 0.2$, $\Delta_p = 0$ (dashed line), $\Delta_v = 0$, $\Delta_p = 0.2$ (dash/dotted line).

Figure 2(a). Critical wavenumbers for plane Couette flow with a less viscous lower fluid. $\Delta_v = \Delta_p = 0$ (dotted line), $\Delta_v = \Delta_p = 0.2$ (solid line), $\Delta_v = \Delta_p = 1$ (dashed line). $r = 1$, $R_1 = 10$, $m < 1$, $G = 0$, $\omega = 1$, $T = 0.01$, $F^{-2} = 0$ and $\delta = 0$.

Figure 2(b). Neutral stability curves for plane Couette flow with a less viscous lower fluid. $\Delta_v = \Delta_p = 0$ (dotted line), $\Delta_v = \Delta_p = 0.2$ (solid line). $\Delta_v = \Delta_p = 1$ (dashed line). Physical parameters are the same as in figure 2(a).

Figure 3. Effect of varying the frequency of oscillatory plane Couette flow. Re σ_{v2} (dashed line), Re σ_{p2} (dashed/dotted line), Re σ_{vp} (solid line).
$r = 1$, $R_1 = 1$, $m = 0.5$, $l_1 = 0.2$, $G = 0$, $F^{-2} = 0$, $T = 0$ and $\delta = 0$.
(a) Long wavelength disturbances, $\alpha = 0.01$,
(b) $O(1)$ wavelength disturbances, $\alpha = 1$,
(c) Short wavelength disturbances, $\alpha = 20$.

Figure 4. The stabilizing/destabilizing effect of the phase difference δ on the growth rates for plane Couette flow. Re σ_s (dotted line), Re σ_{vp} (solid line), Re σ_{v2} (dashed line), Re σ_{p2} (dashed/dotted line). $G = 0$, $\omega = 1$, and $0 < \delta < 2\pi$.
(a) Long wavelength disturbances:

$\alpha = 0.01$, $r = 1$, $R_1 = 10$, $m = 2$, $l_1 = 0.47$ $F^{-2} = 0$ and $T = 0$.
(b) $O(1)$ wavelength disturbances:
$\alpha = 1$, $r = 1$, $R_1 = 10$, $m = 2$, $l_1 = 0.7$, $F^{-2} = 0$ and $T = 0$.
(c) Short wavelength disturbances:
$\alpha = 10$, $r = 2$, $R_1 = 20$, $m = 0.5$, $l_1 = 0.2$, $F^{-2} = 0.1$ and $T = 0.001$.
(d) Short wavelength disturbances:
$\alpha = 20$, $r = 2$, $R_1 = 20$, $m = 0.5$, $l_1 = 0.8$, $F^{-2} = 0.1$ and $T = 0.001$.

Figure 5(a). Critical wavenumbers for oscillating plane Poiseuille flow with a more viscous lower fluid. $\Delta_v = 0$, $\Delta_p = 0$ (dotted line), $\Delta_v = 0.2$, $\Delta_p = 0$ (dashed line), $\Delta_v = 0$, $\Delta_p = 0.2$ (dashed/dotted line), $\Delta_v = 0.2$, $\Delta_p = 0.2$ (solid line), $r = 1$, $R_1 = 10$, $m > 1$, $G = 1$, $\omega = 1$, $F^{-2} = 0$, $T = 0.1$ and $\delta = 0$.

Figure 5(b). Neutral stability curves for oscillating plane Poiseuille flow with a more viscous lower fluid. Physical parameters are the same as in figure 5(a).

Figure 6(a). Stabilizing effect of boundary oscillations for plane Couette-Poiseuille flow. Growth rate as a function of viscosity ratio for a shallower, less viscous, more dense lower fluid: $R_1 = 1$, $l_1 = 0.34$, $\alpha = 1$, $G = 18$, $\omega = 1$, $T = 0.003$, $F^{-2} = 0$, $\delta = 0$, $\Delta_v = \Delta_p = 0.2$ and $r = 4$. Dotted line is Re σ_s, solid line is derived from $\sigma_s + \Delta_v^2\sigma_{v2} + \Delta_p^2\sigma_{p2} + \Delta_v\Delta_p\sigma_{vp}$.

Figure 6(b). Destabilizing effect of boundary/pressure gradient oscillations for plane Couette-Poiseuille flow. Growth rate as a function of viscosity ratio for a deeper, less viscous, less dense lower fluid: $R_1 = 1$, $l_1 = 0.7$, $\alpha = 0.5$, $G = 1$, $\omega = 1$, $T = 0.1$, $F^{-2} = 0.02$, $\delta = 0$, $\Delta_v = \Delta_p = 0.2$ and $r = 0.8$. Dotted line is Re σ_s, solid line is derived from $\sigma_s + \Delta_v^2\sigma_{v2} + \Delta_p^2\sigma_{p2} + \Delta_v\Delta_p\sigma_{vp}$.

Figure 7. Components of growth rate σ as a function of wavenumber α for plane Couette-Poiseuille flow. Lower fluid depths $l_1 = 0.4$ (dotted line), $l_1 = 0.5$ (dashed line), and $l_1 = 0.6$ (solid line). $R_1 = 1$, $m = 0.5$, $G = 1$, $\omega = 1$, $T = 0.001$, $F^{-2} = 0.01$, $\delta = 0$ and $r = 0.5$.

Figure 1(a).

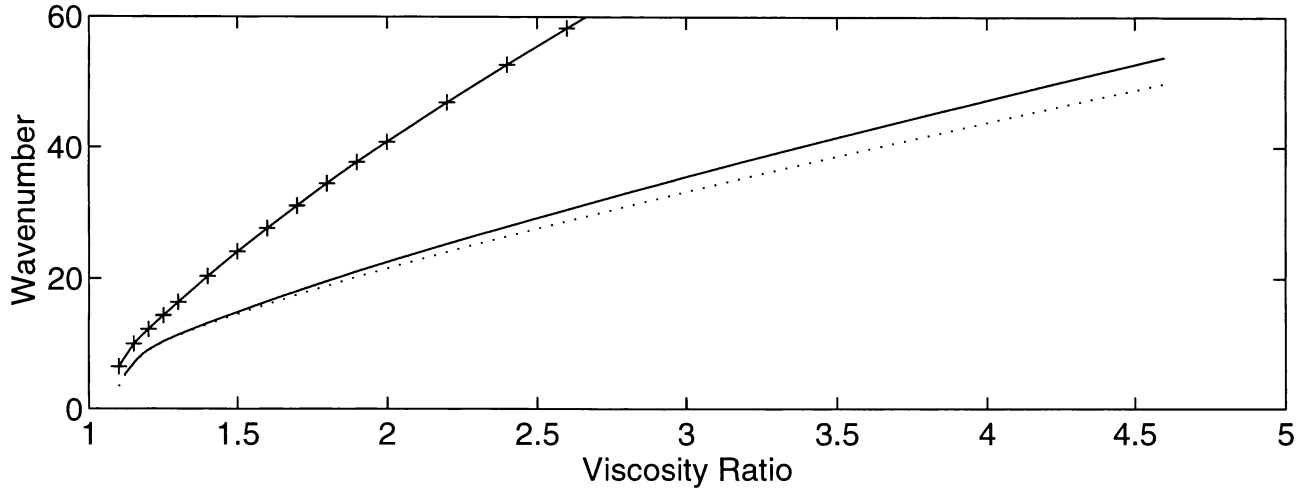

Figure 1(b)

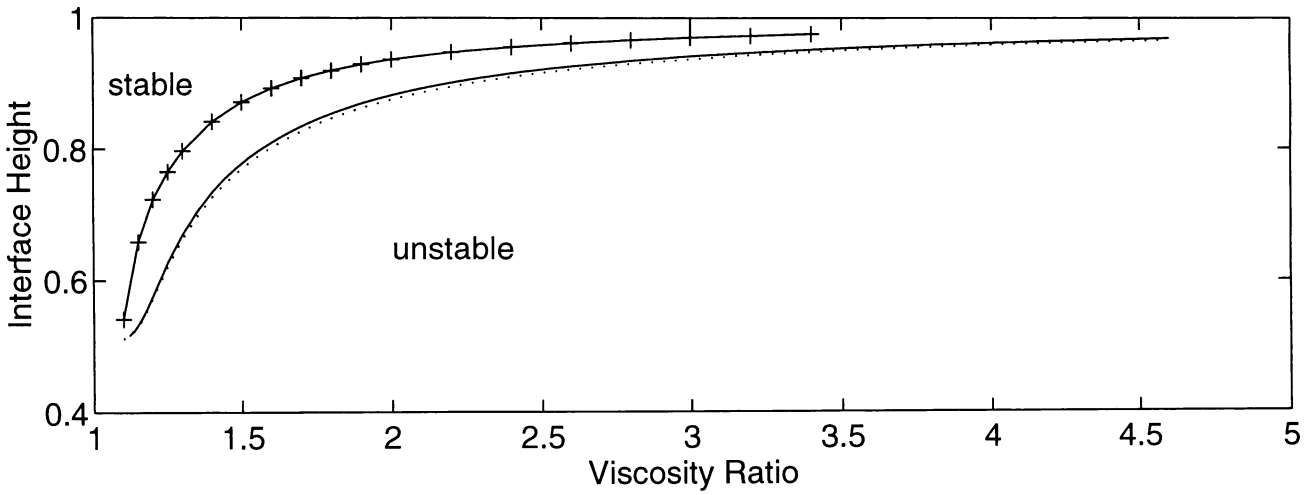

Figure 1(c).

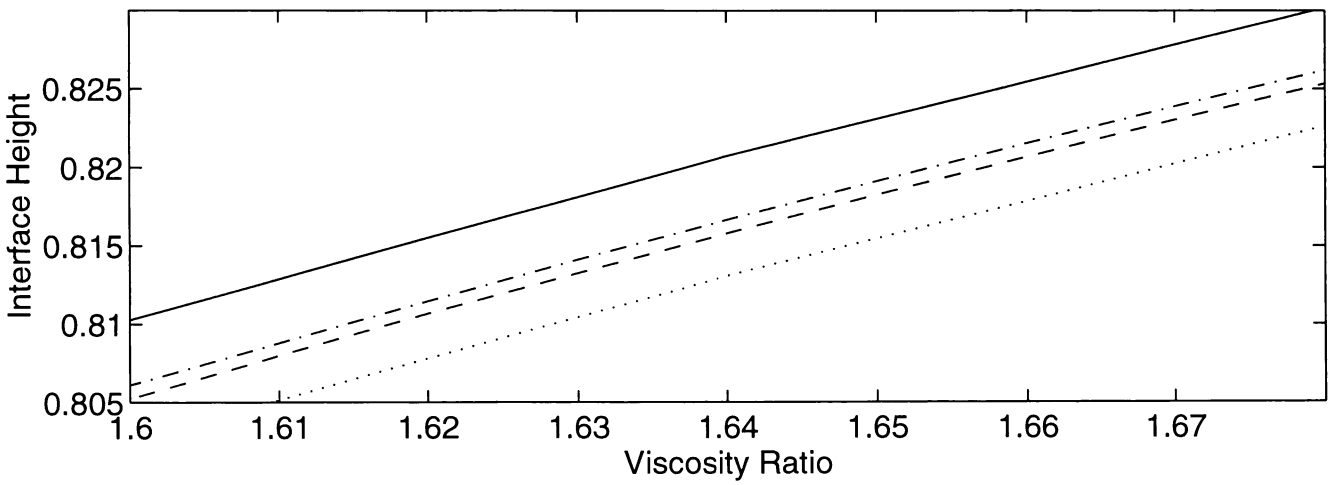
Interface Height
0.825
0.82
0.815
0.81
0.805
1.6
1.61
1.62
1.63
1.64
1.65
1.66
1.67
Viscosity Ratio

Figure 2(a).

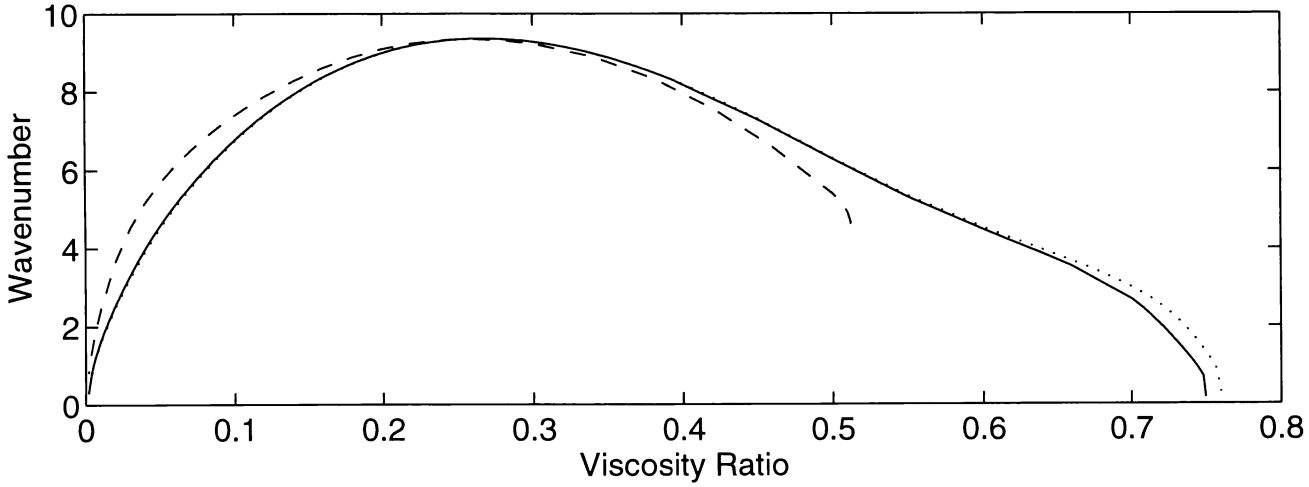

Figure 2(b)

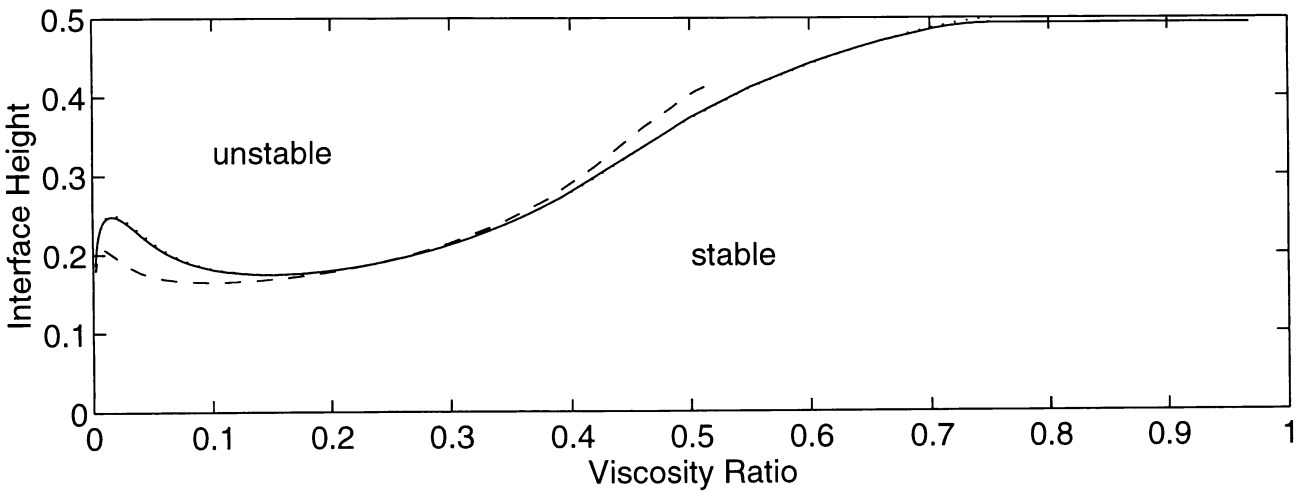

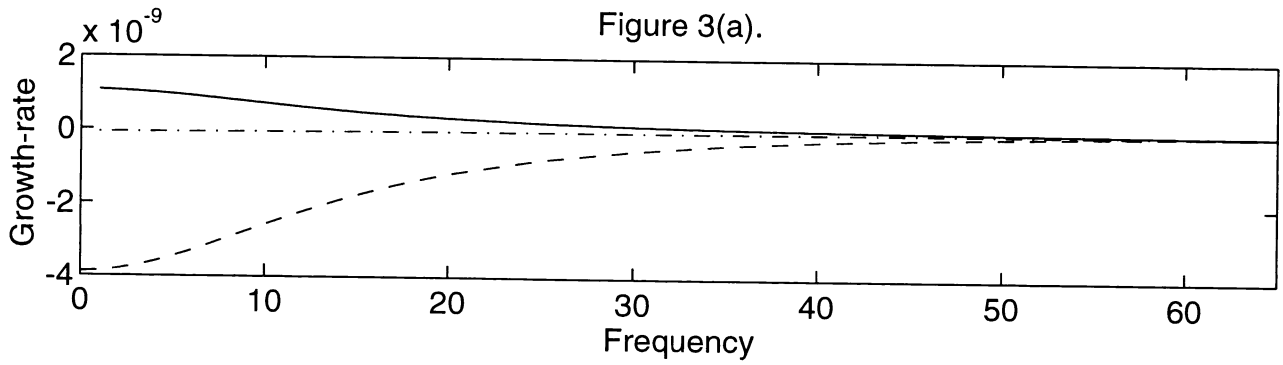

Figure 3(a).

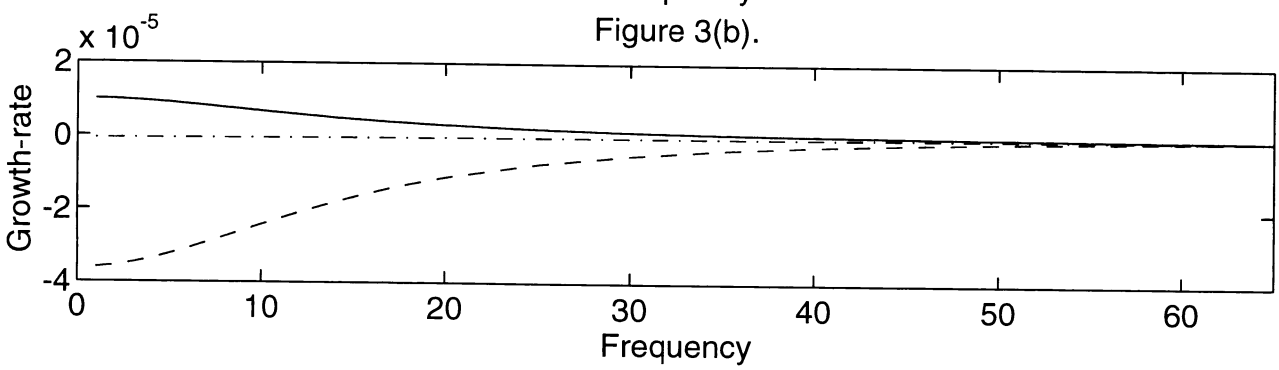

Figure 3(b).

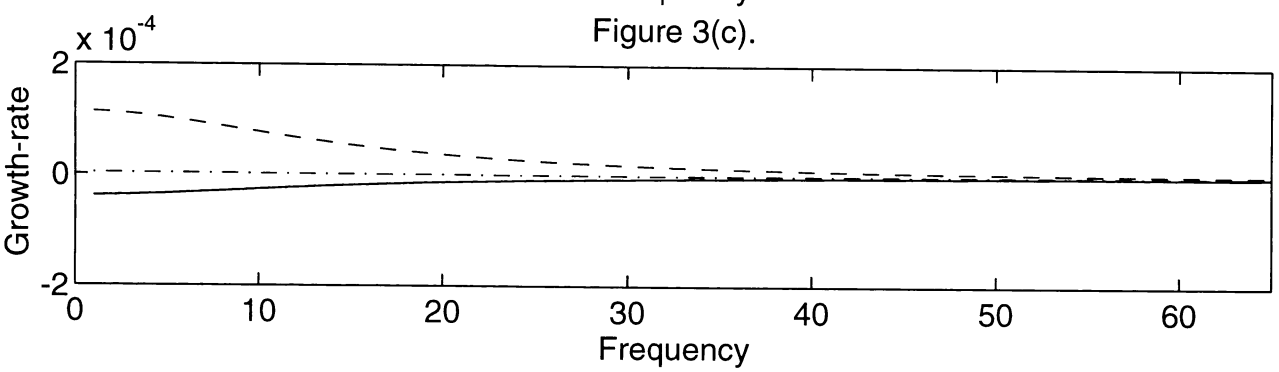

Figure 3(c).

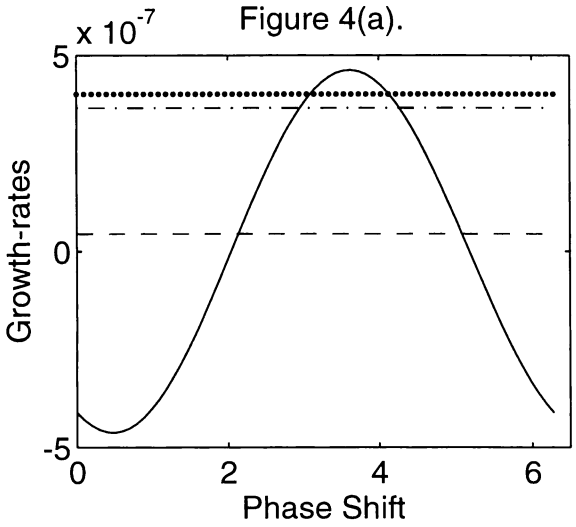

Figure 4(a).

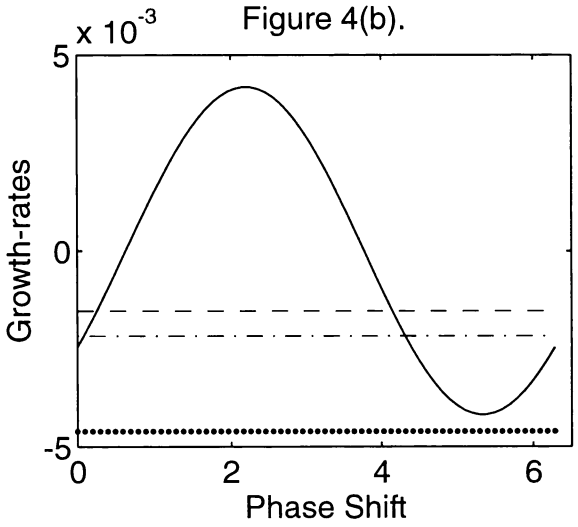

Figure 4(b).

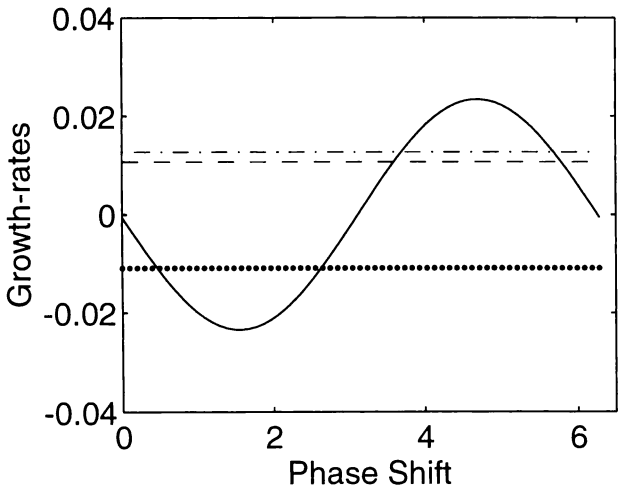

Figure 4(d).

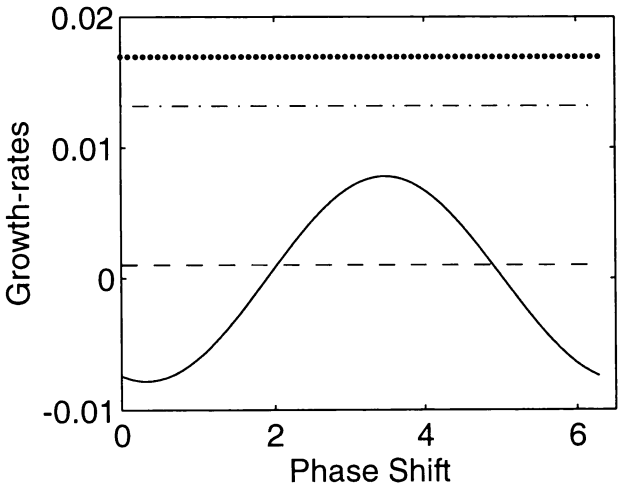

Figure 4(c).

Figure 5(a).

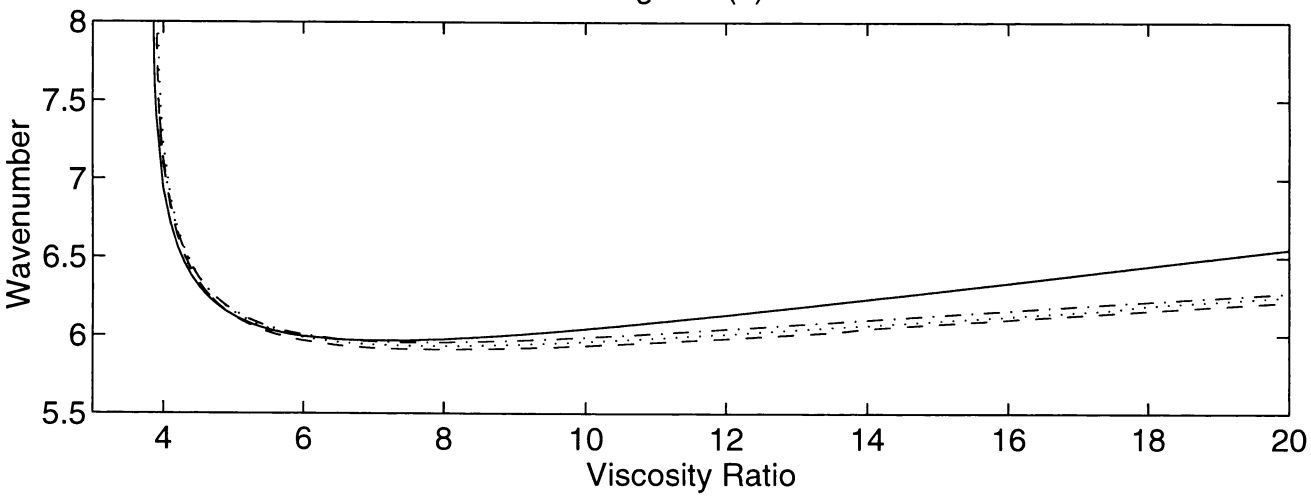

Figure 5(b)

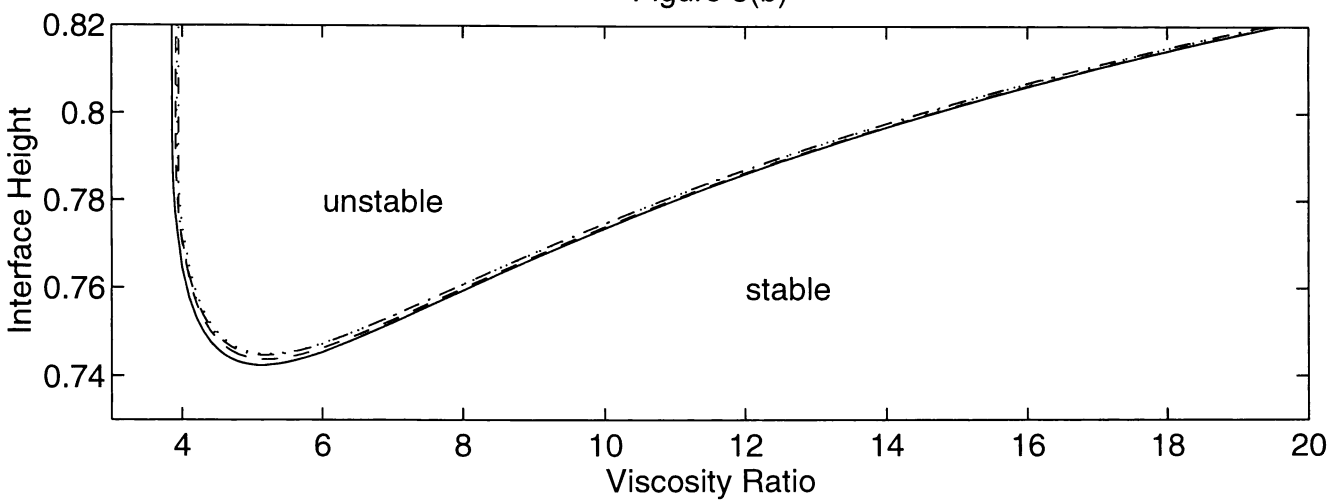

Figure 6(a).

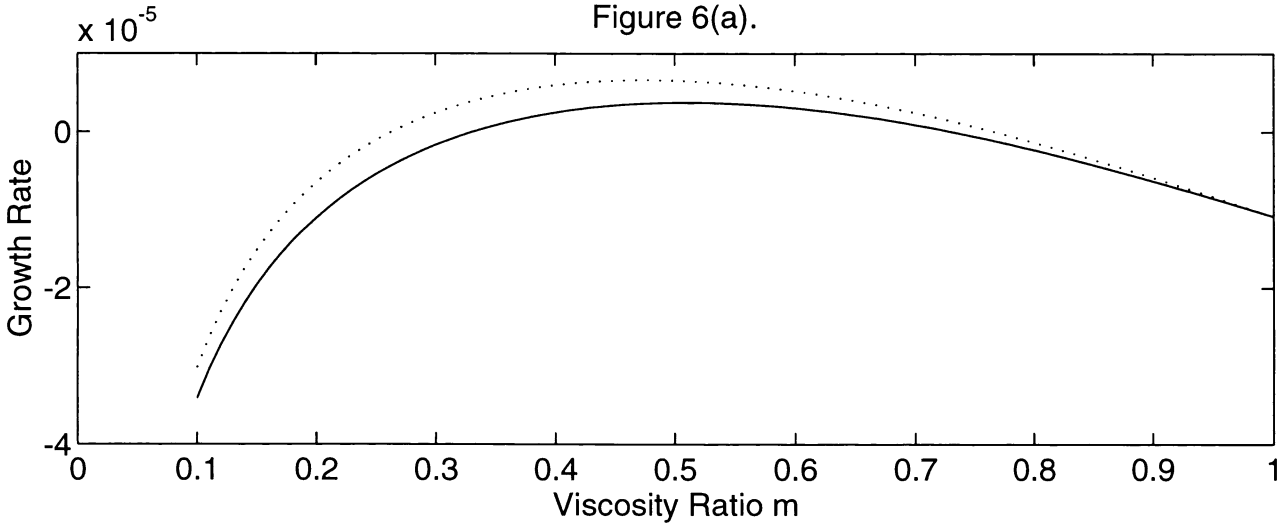

Figure 6(b).

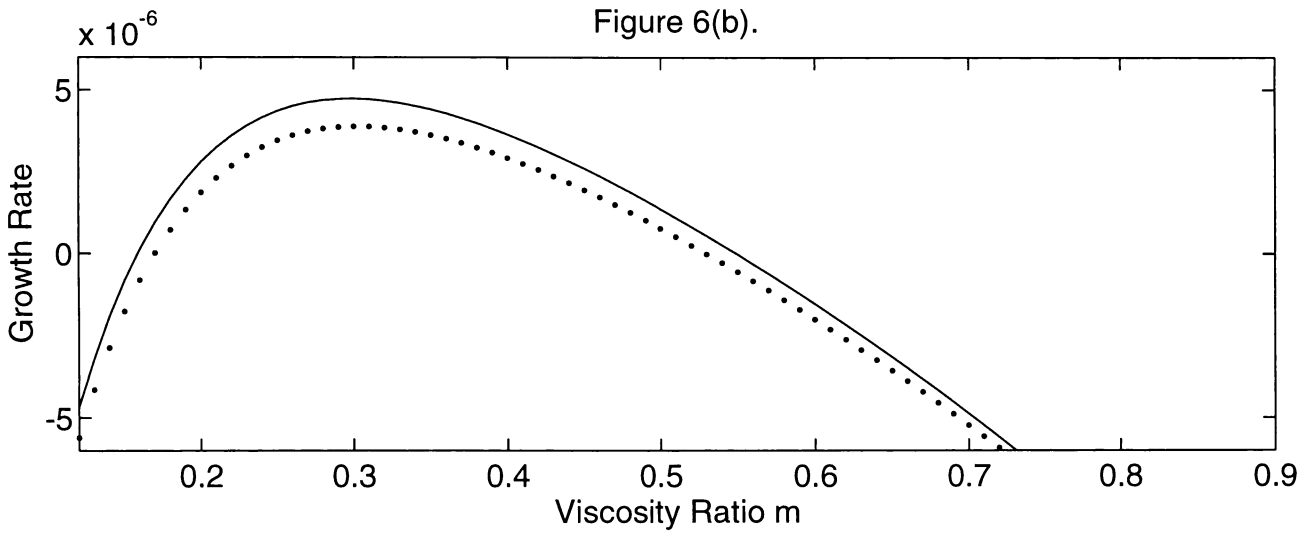

Figure 7.

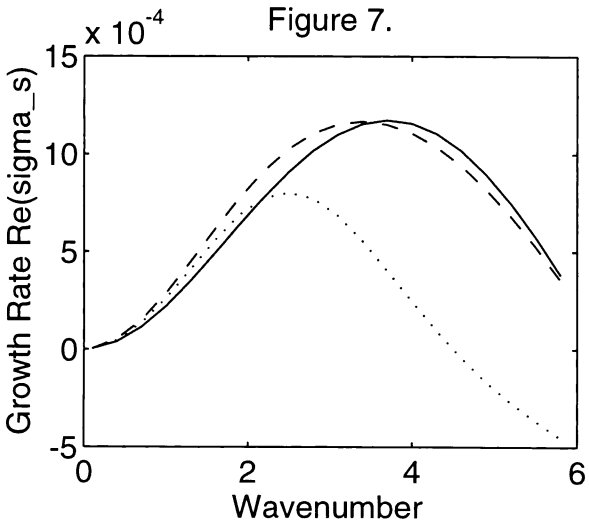
x 10^-4
15
10
5
0
-5
Growth Rate Re(sigma_s)
0
2
4
6
Wavenumber

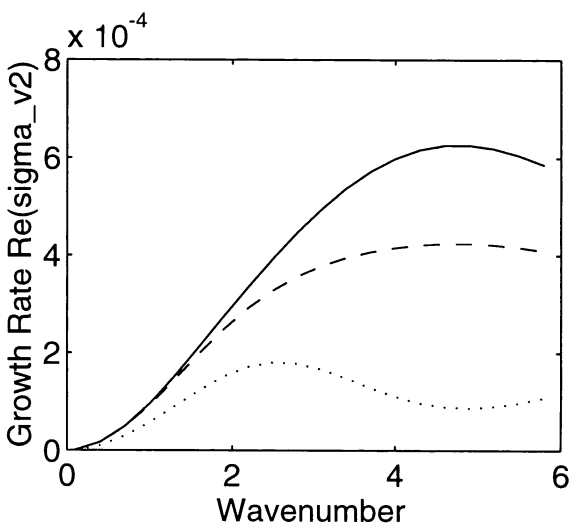
x 10^-4
8
6
4
2
0
Growth Rate Re(sigma_v2)
0
2
4
6
Wavenumber

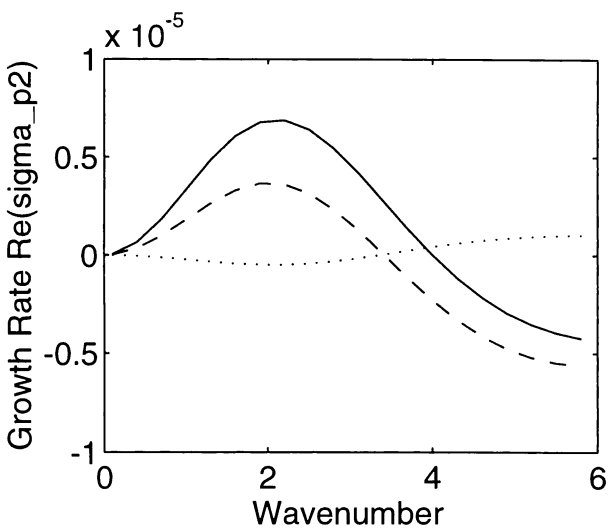
x 10^-5
1
0.5
0
-0.5
-1
Growth Rate Re(sigma_p2)
0
2
4
6
Wavenumber

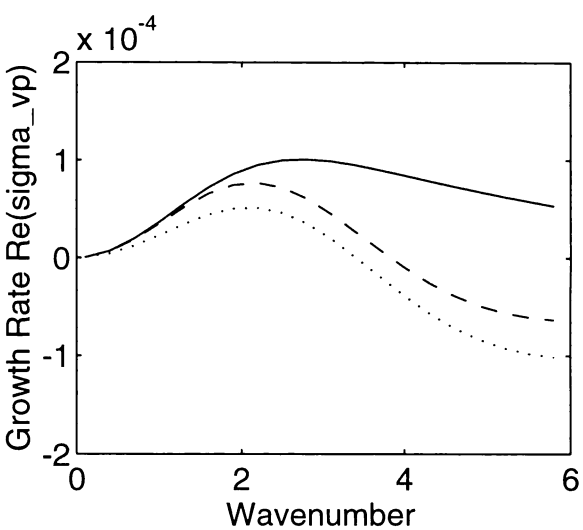
x 10^-4
2
1
0
-1
-2
Growth Rate Re(sigma_vp)
0
2
4
6
Wavenumber

Recent IMA Preprints

#	Author/s	Title

1302 **J. Zhang**, A nonlinear nonlocal multi-dimensional conservation law
1303 **M.E. Taylor**, Estimates for approximate solutions to acoustic inverse scattering problems
1304 **J. Kim & D. Sheen**, A priori estimates for elliptic boundary value problems with nonlinear boundary conditions
1305 **B. Engquist & E. Luo**, New coarse grid operators for highly oscillatory coefficient elliptic problems
1306 **A. Boutet de Monvel & I. Egorova**, On the almost periodicity of solutions of the nonlinear Schrödinger equation with the cantor type spectrum
1307 **A. Boutet de Monvel & V. Georgescu**, Boundary values of the resolvent of a self-adjoint operator: Higher order estimates
1308 **S.K. Patch**, Diffuse tomography modulo Graßmann and Laplace
1309 **A. Friedman & J.J.L. Velázquez**, Liouville type theorems for fourth order elliptic equationsin a half plane
1310 **T. Aktosun, M. Klaus & C. van der Mee**, Recovery of discontinuities in a nonhomogeneous medium
1311 **V. Bondarevsky**, On the global regularity problem for 3-dimensional Navier-Stokes equations
1312 **M. Cheney & D. Isaacson**, Inverse problems for a perturbed dissipative half-space
1313 **B. Cockburn, D.A. Jones & E.S. Titi**, Determining degrees of freedom for nonlinear dissipative equations
1314 **B. Engquist & E. Luo**, Convergence of a multigrid method for elliptic equations with highly oscillatory coefficients
1315 **L. Pastur & M. Shcherbina**, Universality of the local eigenvalue statistics for a class of unitary invariant random matrix ensembles
1316 **V. Jakšić, S. Molchanov & L. Pastur**, On the propagation properties of surface waves
1317 **J. Nečas, M. Ružička & V. Šverák**, On self-similar solutions of the Navier-Stokes equations
1318 **S. Stojanovic**, Remarks on $W^{2,p}$-solutions of bilateral obstacle problems
1319 **E. Luo & H-O. Kreiss**, Pseudospectral vs. Finite difference methods for initial value problems with discontinuous coefficients
1320 **V.E. Grikurov**, Soliton's rebuilding in one-dimensional Schrödinger model with polynomial nonlinearity
1321 **J.M. Harrison & R.J. Williams**, A multiclass closed queueing network with unconventional heavy traffic behavior
1322 **M.E. Taylor**, Microlocal analysis on Morrey spaces
1323 **C. Huang**, Homogenization of biharmonic equations in domains perforated with tiny holes
1324 **C. Liu**, An inverse obstacle problem: A uniqueness theorem for spheres
1325 **M. Luskin**, Approximation of a laminated microstructure for a rotationally invariant, double well energy density
1326 **Rakesh & P. Sacks**, Impedance inversion from transmission data for the wave equation
1327 **O. Lafitte**, Diffraction for a Neumann boundary condition
1328 **E. Sobel, K. Lange, J.R. O'Connell & D.E. Weeks**, Haplotyping algorithms
1329 **B. Cockburn, D.A. Jones & E.S. Titi**, Estimating the number of asymptotic degrees of freedom for nonlinear dissipative systems
1330 **T. Aktosun**, Inverse Schrödinger scattering on the line with partial knowledge of the potential
1331 **T. Aktosun & C. van der Mee**, Partition of the potential of the one-dimensional Schrödinger equation
1332 **B. Engquist & E. Luo**, Convergence of the multigrid method with a wavelet coarse grid operator
1333 **V. Jakšić & C.-A. Pillet**, Ergodic properties of the Spin-Boson system
1334 **S.K. Patch**, Recursive solution for diffuse tomographic systems of arbitrary size
1335 **J.C. Bronski**, Semiclassical eigenvalue distribution of the non self-adjoint Zakharov-Shabat eigenvalue problem
1336 **J.C. Cockburn**, Bitangential structured interpolation theory
1337 **S. Kichenassamy**, The blow-up problem for exponential nonlinearities
1338 **F.A. Grünbaum & S.K. Patch**, How many parameters can one solve for in diffuse tomography?
1339 **R. Lipton**, Reciprocal relations, bounds and size effects for composites with highly conducting interface
1340 **H.A. Levine & J. Serrin**, A global nonexistence theorem for quasilinear evolution equations with dissipation
1341 **A. Boutet de Monvel & R. Purice**, The conjugate operator method: Application to DIRAC operators and to stratified media
1342 **G. Michele Graf**, Stability of matter through an electrostatic inequality
1343 **G. Avalos**, Sharp regularity estimates for solutions of the wave equation and their traces with prescribed Neumann data
1344 **G. Avalos**, The exponential stability of a coupled hyperbolic/parabolic system arising in structural acoustics
1345 **G. Avalos & I. Lasiecka**, A differential Riccati equation for the active control of a problem in structural acoustics
1346 **G. Avalos**, Well-posedness for a coupled hyperbolic/parabolic system seen in structural acoustics
1347 **G. Avalos & I. Lasiecka**, The strong stability of a semigroup arising from a coupled hyperbolic/parabolic system
1348 **A.V. Fursikov**, Certain optimal control problems for Navier-Stokes system with distributed control function
1349 **F. Gesztesy, R. Nowell & W. Pötz**, One-dimensional scattering theory for quantum systems with nontrivial spatial asymptotics
1350 **F. Gesztesy & H. Holden**, On trace formulas for Schrödinger-type operators

1351 **X. Chen**, Global asymptotic limit of solutions of the Cahn-Hilliard equation
1352 **X. Chen**, Lorenz equations, Part I: Existence and nonexistence of homoclinic orbits
1353 **X. Chen**, Lorenz equations Part II: "Randomly" rotated homoclinic orbits and chaotic trajectories
1354 **X. Chen**, Lorenz equations, Part III: Existence of hyperbolic sets
1355 **R. Abeyaratne, C. Chu & R.D. James**, Kinetics of materials with wiggly energies: Theory and application to the evolution of twinning microstructures in a Cu-Al-Ni shape memory alloy
1356 **C. Liu**, The Helmholtz equation on Lipschitz domains
1357 **G. Avalos & I. Lasiecka**, Exponential stability of a thermoelastic system without mechanical dissipation
1358 **R. Lipton**, Heat conduction in fine scale mixtures with interfacial contact resistance
1359 **V. Odisharia & J. Peradze**, Solvability of a nonlinear problem of Kirchhoff shell
1360 **P.J. Olver, G. Sapiro & A. Tannenbaum**, Affine invariant edge maps and active contours
1361 **R.D. James**, Hysteresis in phase transformations
1362 **A. Sei & W. Symes**, A note on consistency and adjointness for numerical schemes
1363 **A. Friedman & B. Hu**, Head-media interaction in magnetic recording
1364 **A. Friedman & J.J.L. Velázquez**, Time-dependent coating flows in a strip, part I: The linearized problem
1365 **X. Ren & M. Winter**, Young measures in a nonlocal phase transition problem
1366 **K. Bhattacharya & R.V. Kohn**, Elastic energy minimization and the recoverable strains of polycrystalline shape-memory materials
1367 **G.A. Chechkin**, Operator pencil and homogenization in the problem of vibration of fluid in a vessel with a fine net on the surface
1368 **M. Carme Calderer & B. Mukherjee**, On Poiseuille flow of liquid crystals
1369 **M.A. Pinsky & M.E. Taylor**, Pointwise Fourier inversion: A wave equation approach
1370 **D. Brandon & R.C. Rogers**, Order parameter models of elastic bars and precursor oscillations
1371 **H.A. Levine & B.D. Sleeman**, A system of reaction diffusion equations arising in the theory of reinforced random walks
1372 **B. Cockburn & P.-A. Gremaud**, A priori error estimates for numerical methods for scalar conservation laws. Part II: Flux-splitting monotone schemes on irregular Cartesian grids
1373 **B. Li & M. Luskin**, Finite element analysis of microstructure for the cubic to tetragonal transformation
1374 **M. Luskin**, On the computation of crystalline microstructure
1375 **J.P. Matos**, On gradient young measures supported on a point and a well
1376 **M. Nitsche**, Scaling properties of vortex ring formation at a circular tube opening
1377 **J.L. Bona & Y.A. Li**, Decay and analyticity of solitary waves
1378 **V. Isakov**, On uniqueness in a lateral cauchy problem with multiple characteristics
1379 **M.A. Kouritzin**, Averaging for fundamental solutions of parabolic equations
1380 **T. Aktosun, M. Klaus & C. van der Mee**, Integral equation methods for the inverse problem with discontinuous wavespeed
1381 **P. Morin & R.D. Spies**, Convergent spectral approximations for the thermomechanical processes in shape memory allows
1382 **D.N. Arnold & X. Liu**, Interior estimates for a low order finite element method for the Reissner-Mindlin plate model
1383 **D.N. Arnold & R.S. Falk**, Analysis of a linear-linear finite element for the Reissner-Mindlin plate model
1384 **D.N. Arnold, R.S. Falk & R. Winther**, Preconditioning in $H(\mathrm{div})$ and applications
1385 **M. Lavrentiev**, Nonlinear parabolic problems possessing solutions with unbounded gradients
1386 **O.P. Bruno & P. Laurence**, Existence of three-dimensional toroidal MHD equilibria with nonconstant pressure
1387 **O.P. Bruno, F. Reitich, & P.H. Leo**, The overall elastic energy of polycrystallin martensitic solids
1388 **M. Fila & H.A. Levine**, On critical exponents for a semilinear parabolic system coupled in an equation and a boundary condition
1389 **J.M. Berg, W.G. Frazier, A. Chaudhary, & S.S. Banda**, Optimal open-loop ram velocity profiles for isothermal forging: A variational approach
1390 **J.M. Berg & H.G. Kwatny**, Unfolding the zero structure of a linear control system
1391 **A. Sei**, High order finite-difference approximations of the wave equation with absorbing boundary conditions: A stability analysis
1392 **A.V. Coward & Y.Y. Renardy**, Small amplitude oscillatory forcing on two-layer plane channel flow
1393 **V.A. Pliss & G.R. Sell**, Approximation dynamics and the stability of invariant sets
1394 **J.G. Cao & P. Roblin**, A new computational model for heterojunction resonant tunneling diode
1395 **C. Liu**, Inverse obstacle problem: Local uniqueness for rougher obstacles and the identification of a ball
1396 **K.A. Pericak-Spector & S.J. Spector**, Dynamic cavitation with shocks in nonlinear elasticity
1397 **G. Avalos & I. Lasiecka**, Exponential stability of a thermoelastic system without mechanical dissipation II: The case of simply supported boundary conditions
1398 **B. Brighi & M. Chipot**, Approximation of infima in the calculus of variations